End-to-End Statistical Model Checking for Parameterization and Stability Analysis of ODE Models

David Julien, Gilles Ardourel, Guillaume Cantin, Benoit Delahaye

End-to-End Statistical Model Checking for Parameterization and Stability Analysis of ODE Models*

DAVID JULIEN, Nantes Université, École Centrale Nantes, CNRS, LS2N, UMR 6004, France
GILLES ARDOUREL, Nantes Université, École Centrale Nantes, CNRS, LS2N, UMR 6004, France
GUILLAUME CANTIN, Nantes Université, École Centrale Nantes, CNRS, LS2N, UMR 6004, France
BENOÎT DELAHAYE, Nantes Université, École Centrale Nantes, CNRS, LS2N, UMR 6004, France

We propose a simulation-based technique for the parameterization and the stability analysis of parametric Ordinary Differential Equations. This technique is an adaptation of Statistical Model Checking, often used to verify the validity of biological models, to the setting of Ordinary Differential Equations systems. The aim of our technique is to estimate the probability of satisfying a given property under the variability of the parameter or initial condition of the ODE, with any metrics of choice. To do so, we discretize the values space and use statistical model checking to evaluate each individual value w.r.t. provided data. Contrary to other existing methods, we provide statistical guarantees regarding our results that take into account the unavoidable approximation errors introduced through the numerical integration of the ODE system performed while simulating. In order to show the potential of our technique, we present its application to two case studies taken from the literature, one relative to the growth of a jellyfish population, and the other concerning a well-known oscillator model.

CCS Concepts: • **Computing methodologies → Model verification and validation**; • **Mathematics of computing → Ordinary differential equations**.

Additional Key Words and Phrases: Statistical model checking (SMC), ordinary differential equations (ODEs), parameterization, stability analysis.

ACM Reference Format:
David JULIEN, Gilles ARDOUREL, Guillaume CANTIN, and Benoît DELAHAYE. 2024. End-to-End Statistical Model Checking for Parameterization and Stability Analysis of ODE Models. *ACM Trans. Model. Comput. Simul.* 1, 1, Article 1 (January 2024), 25 pages. https://doi.org/10.1145/3649438

1 INTRODUCTION

All scientific branches share the common concept of modeling. When scientists study a real-life system, the first step they go through is to build a model that gathers all the existing knowledge of the target system. This model is then used as a proxy of the system it represents in order to analyze it and perform simulation or predictions. In several fields, such as Biology, Chemistry, Physics or Engineering, models do not represent a single system but are instead an abstraction for a *family* of systems that share common traits but might exhibit some internal variability. This internal variability can either be left out by considering that the model represents the "average"

*This work is partially supported by ANR BisoUS (ANR-22-CE48-0012) and research project VERHYDYN (Verification of Hybrid Dynamical Systems) funded by INS2I-CNRS.

Authors' addresses: David JULIEN, david.julien@univ-nantes.fr, Nantes Université, École Centrale Nantes, CNRS, LS2N, UMR 6004, Nantes, France, F-44000; Gilles ARDOUREL, Nantes Université, École Centrale Nantes, CNRS, LS2N, UMR 6004, Nantes, France, F-44000; Guillaume CANTIN, Nantes Université, École Centrale Nantes, CNRS, LS2N, UMR 6004, Nantes, France, F-44000; Benoît DELAHAYE, Nantes Université, École Centrale Nantes, CNRS, LS2N, UMR 6004, Nantes, France, F-44000.

individual in the family, or taken into account inside the model through the use of non-determinism, probabilities or parametricity.

There are two main factors that can have an important effect on the behavior of a given parametric model: the value of the parameter and the value of the initial condition. The process of choosing the right parameter value is called parameterization: it consists in confronting the model with a given set of observations of the (family of) system(s) it represents in order to find the parameter values that best fit this (family of) system(s). In most cases, parameterization techniques are *deterministic* [40]. They lead to deterministic parameter values that best fit the experimental data, i.e. that produce the best fit for the "average" individual. In this paper, we instead focus on a technique that allows to select parameter values that best fit *under variability*, i.e. that produce the best *probabilistic* fit for the *whole family*. Once an adequate parameter value has been chosen, scientists often study the impact of the value of the initial condition on the behavior of the model. In this context, one issue of interest is stability: an equilibrium point x_e is called *stable* if the forward orbit of any point near x_e stays in its vicinity. Stability may be a local or global property of the state space. In this paper, we propose a technique that again takes advantage of internal variability in order to study the stability of a given model.

Symbolic techniques such as parametric model checking [3, 10] are often difficult to use in practice because they require automata-based models while real-life models are often expressed either with computer programs or with differential equation models. Statistical Model Checking (SMC) [26], however, can be applied to any stochastic model for which simulations can be performed. It is a simulation-based technique that allows to estimate, with formal guarantees, the probability that a given (probabilistic) model satisfies a given property.

Parameterization, or *parameter synthesis* has been the topic of many works in the context of probabilistic systems [11, 16, 17, 19, 25]. SMC has been successfully applied to perform parameterization of real-life models expressed using several formalisms such as parametric Markov chains [4], parametric Python programs [39], or even parametric Ordinary Differential Equation (ODE) systems [27]. To the best of our knowledge, SMC techniques have never been used in the context of stability. Nevertheless, symbolic techniques have been used in the context of deterministic or stochastic hybrid systems where they are applied directly on the system [15, 37], or on an abstraction graph [38], to assess the stability of a given model. By adapting SMC to ODE models, we enable the analysis of their stability *under variability*, thus extending the application domain of model stability analysis to models on which experiments can be performed.

Unfortunately, the formal guarantees obtained through SMC are linked to the simulation space (i.e. the produced traces) and not to the original model itself. When the model consists in sets of ODEs, as in [27], numerical integration methods are used in order to solve the ODEs and perform simulations, which means that the formal guarantees obtained through SMC cannot apply to the original ODE model because of the approximations introduced in the process.

The resolution of ODE systems has been the subject of extensive study. More precisely, integration methods such as implicit and explicit Runge-Kutta (which we use in this article) have been validated [1] to guarantee the precision of the computations and thus the validity of reachability properties on initial values of the system. Moreover, these techniques may be extended to the *set initial value problem* [2], allowing to guarantee the computation on a set of initial values, thus assessing reachability properties on the whole set. These techniques have been implemented in ODE solvers such as VNODE-LP and GRKLib [6, 34], which solve ODEs while taking into the account the approximation errors accumulated in the process. Another approach relies on the property of the measure of the system's Jacobian [30]. Finally, rigorous approaches have been developed [41, 43] to merge SMC techniques with ODE resolution. To the best of our knowledge, in these papers, the guarantees regarding integration errors are not linked to the integration method or the integration

step. In this work, in addition to the guarantees regarding integration errors for the whole set of values, we study the link between the error and the integration step and provide, in some cases, a way to compute the integration step ensuring a given bound is respected.

In this paper, our contribution is to bridge the gap between the original ODE model and the results of the SMC procedure by *combining the statistical guarantees of SMC with the global approximation error of standard numerical integration methods*, both in the case of parameterization and in the case of stability analysis. As in [27], we consider ODE models with structural parameters. We build on the logic proposed in [27] to express our properties of interest and also consider expected-reward properties that might be of interest in practice. We use SMC to evaluate values by estimating the expectation of a given reward function for these values while taking internal variability into account. Contrarily to what is done in [27], the accuracy of this estimation is guaranteed w.r.t. the original ODE model. In the case of structural parameters, it enables the parameterization of the model, so that the trace of the model fits best with given experimental data by staying within a tunnel of arbitrary radius around the data. In the case of initial conditions, it enables the study of the associated Cauchy problem, especially the analysis of the stability of the system w.r.t. the initial condition; to this end, we introduce a bounded definition of stability by requiring the trace to stay at an arbitrary distance from the data for an arbitrary amount of time.

To illustrate our results, we perform the parameterization of a state-of-the-art model taken from the literature using our technique, as well as a study on the stability of the initial condition of a well-studied oscillator model. In this context, and because modelers are often interested by this information in practice, we propose a global evaluation of the value spaces that allows us to get a complete picture of the adequacy of the values w.r.t. the given data. Nevertheless, our results are generic and could be applied to any search technique, such as the local ones performed in [27].

Intuition. To give an intuition of our contribution, we provide an informal summary of the method we present in this paper in the context of parameterization, although the method is the same in the context of stability analysis. Recall that, given a dataset and a parametric ODE system, the objective is to find a solution to a parametric ODE system (i.e. a parameter value) that satisfies a property φ w.r.t. the dataset, which is, given a distance $\delta > 0$, "the solution stays in a tunnel of radius δ around the data" [1]; we also want to acquire statistical guarantees on said result. The main issue is that we can only simulate our model by solving the ODE system using numerical integration methods. Hence, we cannot directly verify whether exact solutions (x) of the system satisfy φ and instead have to rely on approximate solutions (y). We therefore proceed as follows: we start by discretizing the set of parameter values into a grid; we then evaluate each point of this grid using the procedure detailed below; finally, we use the resulting scores to select the "best" parameter values w.r.t. φ. The score of a given parameter value $\boldsymbol{\lambda}$ is computed as follows, and illustrated in Figures 1 and 2 in the context of the case study presented in Section 3.4.

(1) We set the parameter value to $\boldsymbol{\lambda}$. Through a careful study of the ODE system, we give a bound on the distance ε between exact (x) and approximate (y) solutions. We emphasize that this bound depends on (i) the chosen integration technique and (ii) the chosen integration step. We show that this distance is uniformly stable w.r.t. internal variability around $\boldsymbol{\lambda}$, but also that it can be uniformly bounded on the global set of solutions (i.e. independently of $\boldsymbol{\lambda}$).
(2) We propose two new properties φ_- and φ_+ that will be verified on the approximate solutions y, and depend on the above distance. This amounts to changing the size of the tunnel around the experimental dataset. We compute (estimations of) the respective probabilities p_- and p_+ and prove that the probability p that x satisfies φ lies between p_- and p_+.

[1] In the context of stability, given an interval $[T_1, T_2]$ of time, the property is "the solution stays in a tunnel of radius δ around the equilibrium between time points T_1 and T_2."

(3) We provide statistical guarantees of our estimation, i.e. a confidence interval for our estimation of p, and use this estimation as the score for parameter value $\boldsymbol{\lambda}$.

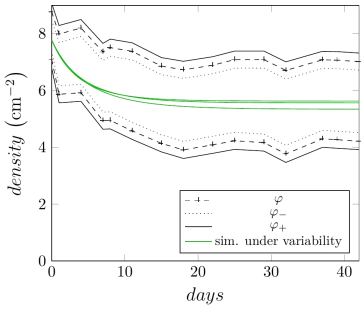

Fig. 1. Tunnels corresponding to the properties $\varphi, \varphi_-, \varphi_+$ and accepted simulations.

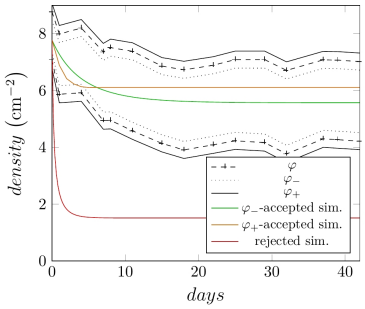

Fig. 2. φ_--accepted, φ_+-accepted and rejected simulations.

It is worth noting that the underlying theory is generic: the integration method as well as the statistical estimation method can be chosen arbitrarily as long as they provide the usual guarantees. In this paper, we use Runge-Kutta and Monte-Carlo for the sake of example. We also emphasize that the nature of the problem is arbitrary: we chose two examples from the literature to have references regarding the consistency of the results, but this method may be applied to *any* well-defined ODE model, including systems for which the symbolic analysis proves too complicated, for instance in the case of systems of high order. Moreover, the method being generic makes it readily usable for hybrid systems.

Outline. In Section 2, we introduce the definitions and notations to be used later in this article, regarding both the logical and mathematical aspect. In Section 3, we state the first of our two results, i.e. we provide the statistical guarantees for the estimation of the probability of satisfaction of a property related to the structural parameter of an ODE. In Section 4, we state the second result of the paper, i.e. we extend the study of the ODE parameter to that of the initial condition of a Cauchy problem, and provide a method to experimentally exhibit basins of attraction around an equilibrium. Finally, we conclude in Section 5 and give perspectives for future work.

Remark. This article is an extension of a conference article [24], in which only the parameterization problem was addressed. Here, we extend our study to the context of stability analysis. In this context, we consider variations of the initial condition of the Cauchy problem associated with an ODE model instead of the parameter of the model, and show that one can also bound the approximation error during the ODE integration so that formal guarantees can be obtained and SMC techniques can be applied.

2 DEFINITIONS AND NOTATIONS

We begin with recalling definitions and introducing notations. Then, we will present the logic used in this paper and extend it by introducing reward functions.

2.1 ODE preliminaries

In this paper, we consider evolution problems described by an Ordinary Differential Equation (ODE) of the form

$$\frac{\mathrm{d}x(t)}{\mathrm{d}t} = f\big(x(t), \boldsymbol{\lambda}\big), \quad t > 0. \tag{1}$$

In Equation (1), the unknown function x is defined in $\mathbb{R}^+$ with values in $\mathbb{R}^n$; $\boldsymbol{\lambda} \in \mathbb{R}^m$ is a parameter vector of real values; f is a function defined on $\mathbb{R}^n \times \mathbb{R}^m$ with values in $\mathbb{R}^n$, whose regularity will be detailed below; n, m are positive integers. In the following, we write $x_i(t)$, $1 \leq i \leq n$, for the projection of $x(t)$ on its ith component. As mentioned in our introduction, Equation (1) can model various real-world problems arising in life sciences. Our goal is to study some properties of the trajectories determined by Equation (1), by developing an innovative statistical model-checking framework suitable for the continuous dynamics of ODEs. It consists mainly in the comparison of two sets of points: a data set—which may or may not be experimental data—, and the set of states computed from traces of the model. Hence, these methods not only apply to the parameterization of models and comparison with data (as seen in Section 3.4), but also to the comparison with theoretical studies (as seen in Section 4.3).

Standard results of the theory of differential equations (see for instance [35]) ensure that, for any value of the parameter $\boldsymbol{\lambda} \in \mathbb{R}^m$, the Cauchy problem determined by Equation (1) and an initial value $x(0) = x_0 \in \mathbb{R}^n$ admits a unique solution, provided f is C^1 on $\mathbb{R}^n \times \mathbb{R}^m$; we denote by $x(t, x_0, \boldsymbol{\lambda})$ the corresponding trajectory, which we assume to be defined on $[0, T]$ with $T > 0$. If the context is sufficiently clear, we may write $x(t)$ for short. As before, we write $x_i(t, x_0, \boldsymbol{\lambda})$ (resp. $x_i(t)$), $1 \leq i \leq n$, for the projection on its ith component. We assume that the component λ_j of the parameter vector $\boldsymbol{\lambda} \in \mathbb{R}^m$ ($1 \leq j \leq m$) satisfies $\lambda_j \in [L_j^{\boldsymbol{\lambda}}, U_j^{\boldsymbol{\lambda}}]$, with real coefficients $L_j^{\boldsymbol{\lambda}} < U_j^{\boldsymbol{\lambda}}$, and that the trajectories of Equation (1) admit a rectangular invariant region, uniform w.r.t. the parameter $\boldsymbol{\lambda}$, that is $x_i(t, \boldsymbol{\lambda}) \in [L_i, U_i]$ for $t \in [0, T]$, with real coefficients $L_i < U_i$, for any parameter $\boldsymbol{\lambda}$ and for $1 \leq i \leq n$. The global invariant region for x is written $\mathbf{V}$, the parameter space is written $\mathbf{W}$. These spaces, along with a new set INIT, are defined as follows:

$$\mathbf{V} = \prod_{i=0}^{n} [L_i, U_i] \qquad (2) \qquad \mathbf{W} = \prod_{j=0}^{m} [L_j^{\boldsymbol{\lambda}}, U_j^{\boldsymbol{\lambda}}] \qquad (3) \qquad \mathsf{INIT} = \mathbf{V} \times \mathbf{W}. \qquad (4)$$

For $a \in \mathbf{V}$, we consider the Euclidian norm defined on $\mathbb{R}^n$ by $\|a\|_{\mathbb{R}^n} = \left(\sum_{i=1}^{n} a_i^2\right)^{\frac{1}{2}}$. Similarly, for $\boldsymbol{\lambda} \in W$, we consider the Euclidian norm defined on $\mathbb{R}^m$ by $\|\boldsymbol{\lambda}\|_{\mathbb{R}^m} = \left(\sum_{j=1}^{m} \left|\lambda_j\right|^2\right)^{\frac{1}{2}}$.

Finally, we write TRAJ for the set of all potential trajectories of the solutions to our ODE system. Formally, $\mathsf{TRAJ} = \{x(t, x_0, \boldsymbol{\lambda}) \mid x_0 \in \mathbf{V}, \boldsymbol{\lambda} \in \mathbf{W}$ and x is a solution to Equation (1)$\}$.

It is well-known that Equation (1) determines time continuous trajectories, which moreover depend continuously on a variation of the initial condition $x_0 \in \mathbf{V}$ and of the parameter $\boldsymbol{\lambda} \in \mathbf{W}$ (see for instance [35]). In Section 3, we will be interested in the variation of those trajectories under a variation of the parameter $\boldsymbol{\lambda} \in \mathbf{W}$, while in Section 4 we will be interested in the variation of those trajectories under the variation of the initial condition $x_0 \in \mathbf{V}$. We now move to the description of the Σ-algebra used for the statistical verification of our models.

2.2 Definition of the Σ-algebra

As explained in the introduction, our aim is to study the behavior of an ODE system under the variation of its structural parameter or its initial condition (i.e. its initial state). This consists in verifying that the studied model satisfies a given property. Since our verification is intrinsically experimental, we have to define a finite set of time points at which we will check the satisfaction of said property, in the following manner:

$$\mathcal{T} = \{0 = t_0, t_1, \ldots, t_k = T\}. \qquad (5)$$

Furthermore, we assume the existence of a set of q observations—numerical values—for each time point $t \in \mathcal{T}$ and for each coordinate $0 \leq i \leq n$. We assume, in practice, that $\mathcal{T}$ indeed includes all the time points where observations are available. Remark nonetheless that $\mathcal{T}$ is not necessarily

limited to this set, as we could have an empty set of observations for a number of $t \in \mathcal{T}$. Since $\mathcal{T} = \{t_0, \dots t_k\}$ is finite, we abuse notations and substitute it, when convenient, with the integer set $\mathcal{T} = \{0, \dots k\}$.

We call "property" a measurable set of traces. In this paper, we consider a property Ψ given along with a decision procedure regarding its satisfiability, and we identify through $\mathsf{models}(\Psi) = \{x \in \mathsf{TRAJ} \mid x \in \Psi\}$ the set of trajectories which satisfy Ψ. Note that since Ψ can be seen as both a property and a set of trajectories, we sometimes use the wording "x satisfies Ψ" instead of "$x \in \Psi$", depending on the context.

Since our aim is to consider variability on the ODE models of interest, we may use statements of the form $\mathbb{P}_{\geq p}(\Psi)$, whose interpretation is expressed as follows: "the probability that a trajectory in TRAJ is in $\mathsf{models}(\Psi)$ is greater than p". In this regard, we need to define a probability measure $\mathbb{P}$ over TRAJ.

We notice that the pair $(x_0, \boldsymbol{\lambda})$ completely determines the trajectory $x(x_0, \boldsymbol{\lambda}) \in \mathsf{TRAJ}$ (see [18]). Consequently, TRAJ can be completely identified with INIT, defined in Equation (4). Formally, we define $\mathsf{Models}(\Psi) \subseteq \mathsf{INIT}$ as the set

$$\{(x_0, \boldsymbol{\lambda}) \in \mathsf{INIT} \mid x(t, x_0, \boldsymbol{\lambda}) \in \mathsf{models}(\Psi)\} \tag{6}$$

and consider the Σ-algebra $\mathscr{B}$ generated by the $(n \times m)$-dimensional open intervals of INIT. As expected, $\mathscr{B}$ is an adequate support to prove the measurability of $\mathsf{Models}(\Psi)$ for a property Ψ expressed through classical logics.

Depending on the context, we will use the Σ-algebra $\mathscr{B}^{\mathbf{W}}$ when studying the parameter values $\boldsymbol{\lambda} \in \mathbf{W}$, in which case $\mathsf{INIT} = \{x_0\} \times \mathbf{W}$ for a fixed $x_0 \in \mathbf{V}$, and $\mathscr{B}^{\mathbf{V}}$ when studying the initial conditions $x_0 \in \mathbf{V}$, in which case $\mathsf{INIT} = \mathbf{V} \times \{\boldsymbol{\lambda}\}$ for a fixed $\boldsymbol{\lambda} \in \mathbf{W}$.

In the following, we will consider a number of probability distributions $\mathbb{P}$ on $\mathscr{B}$ (one for each parameter pair $(x_0, \boldsymbol{\lambda})$), and use these probability distributions to evaluate whether our ODE model meets a specification of the form $\mathbb{P}_{\geq p}(\Psi)$. This will amount to checking whether $\mathbb{P}(\mathsf{Models}(\Psi)) \geq p$: we will use SMC to estimate the proportion of satisfactory trajectories in INIT.

In our context, each pair $(x_0, \boldsymbol{\lambda}) \in \mathsf{INIT}$ will give rise to a probability distribution $\mathbb{P}$ taking into account internal variability either on the parameter $\boldsymbol{\lambda} \in \mathbf{W}$ or the initial condition $x_0 \in \mathbf{V}$. For convenience, and since we study only one member of a pair at once, we will identify each pair with the relevant member, and anotate the probability $\mathbb{P}$ accordingly: $\mathbb{P}^{\boldsymbol{\lambda}}$ when we study the influence of the structural parameter $\boldsymbol{\lambda}$, and $\mathbb{P}^{x_0}$ when we study the influence of the initial condition x_0.

This probability distribution will be used to evaluate the model against the property Ψ, which will yield a score written $\mathsf{grade}(x_0, \boldsymbol{\lambda})$ that represents the adequacy of the trace induced by the pair $(x_0, \boldsymbol{\lambda})$ w.r.t. the given data while taking into account internal variability.

However, it might happen that many of the pairs $(x_0, \boldsymbol{\lambda})$ in the INIT set have a maximal score $\mathsf{grade}(x_0, \boldsymbol{\lambda}) = 1$, i.e. satisfy the formula $\mathbb{P}_{\geq 1}(\Psi)$. This could be the case if all the traces generated using $\mathbb{P}$ satisfy the property Ψ. In this case, we will need to consider more complex properties to sort those values and filter them. To this purpose, we introduce the notion of reward function.

2.3 Reward functions

The purpose of statistical model checking in general, and the Monte-Carlo method in particular, which will be presented in detail in Section 3.2, is to estimate with formal guarantees the expected value of a given function on a measurable set. In the context of model checking, this procedure is used to estimate the probability that a given model satisfies a property. To do this, a great number of samples is produced, each sample of the system is checked against the property and a Boolean reward is computed accordingly (i.e. 1 if the property is satisfied and 0 otherwise). Statistical model

checking then amounts to estimating the expected value of this particular reward function on the measurable set of traces of the model at hand.

In our case, this boils down to defining a reward function $r_\Psi : \mathsf{TRAJ} \to \{0, 1\}$ that evaluates to 1 on a trajectory $x \in \mathsf{TRAJ}$ if the trajectory satisfies Ψ and 0 otherwise. Statistical model checking will then compute an estimation of the expected value of r_Ψ on the set of traces TRAJ under the probability distribution $\mathbb{P}$, which in the end will be an estimation of the measure of $\mathsf{Models}(\Psi)$ for the pair $(x_0, \boldsymbol{\lambda})$.

In order to evaluate the pair $(x_0, \boldsymbol{\lambda})$ in a more discriminating way, we allow the use of non-Boolean reward functions. This allows us to express more powerful properties than those that can be defined using classical logics. For instance, one can use those reward functions in order to measure the number of time points for which the current trace does not agree with the given observations, or to measure the cumulative distance between the trace and the observations at all time points.

In the following, we will therefore consider a given reward function $r : \mathsf{TRAJ} \to \mathbb{R}$ and use statistical model checking to estimate its expected value on the trajectories of our model under a given probability distribution $\mathbb{P}$. When convenient, we will identify a given property Ψ with its associated reward function obtained through the above construction r_Ψ.

3 STATISTICAL MODEL CHECKING FOR PARAMETERIZATION

In this section, we state our first result: we provide statistical guarantees on the verification of specific properties under variation of the parameter $\boldsymbol{\lambda}$. More specifically, given a property φ (resp. the corresponding reward function r_φ) on the trajectories of Equation (1), we will establish confidence intervals regarding the estimation of the *probability* of satisfaction of that property (resp. the *expected value* of r_φ), which shall be computed using *approximate solutions* to Equation (1), as well as a bound on the errors w.r.t. the *exact probability* corresponding to the *exact solutions* to Equation (1). We then illustrate our approach with a case study taken from the literature, by parameterizing the proposed model.

Note that we focus on the structural parameter $\boldsymbol{\lambda}$: from here and until the end of the section, we declare x_0 to be a constant equal to the first observation of the studied system. As indicated in Section 2.2, we will identify the pair $(x_0, \boldsymbol{\lambda}) \in \mathsf{INIT}$ to $\boldsymbol{\lambda}$.

3.1 Approximation method for the numerical integration of the ODE

We recall that an approximation method, which determines the approximate solution $y(t, x_0, \boldsymbol{\lambda})$ to the ODE induced by parameter $\boldsymbol{\lambda}$ and initial condition x_0, can be written

$$y(0) = x_0, \quad y(\tau_{j+1}) = y(\tau_j) + h\,\Phi\big(\tau_j, y(\tau_j), \boldsymbol{\lambda}, h\big), \quad 0 \leq j < J, \tag{7}$$

where Φ is a continuous function defined in $[0, T] \times \mathbb{R}^n \times \mathbf{W} \times \mathbb{R}$ with values in $\mathbb{R}^n$, τ_j are the discrete points of definition of y, and $h \in \mathbb{R}^+$ is the integration step. Intuitively, those methods compute each point thanks to the previous one. In this paper, we use the well-known Runge-Kutta 4 method, which is a standard method for ODE integration, though this technique may be extended to any integration method whose integration step is bounded—which is always the case when integrating on finite intervals.

For the sake of simplicity, we focus in the following on the theoretical study of 1-dimensional systems ($n = 1$), but our method can be adapted to larger systems ($n \geq 2$) as shown in our second case study presented in Section 4.3, mostly by adapting the definition of distance introduced below.

As explained in Section 2.2, we consider a set γ of observations, recorded at $(k + 1, k \geq 0)$ time points forming a set $\mathcal{T}$ (see Equation (5)) with values in $\mathbb{R}^n$. We start by defining a notion of distance between functions that will, in the end, allow us to compare the solutions of our ODE model with

the given set of observations. Given any two functions g_1, g_2 in the set $F_{\mathcal{T}} = \{g : I \to \mathbb{R} \mid \mathcal{T} \subseteq I\}$, where I denotes an interval included in $\mathbb{R}$, we consider the distance d defined by

$$d(g_1, g_2) = \max_{t \in \mathcal{T}} |g_1(t) - g_2(t)| . \tag{8}$$

Note that d is rigorously only a *pseudo*-distance, since two functions g_1 and g_2 defined on $[0, T]$, that are distinct on $[0, T]$, might coincide on the finite set $\mathcal{T}$, thus could satisfy $d(g_1, g_2) = 0$. Nevertheless, since our purpose is to measure the distance to the set of observations γ, we do not need to distinguish such two functions. Moreover, one may use any arbitrary (pseudo-)distance, since all norms are equivalent in the finite-dimensional space $\mathbb{R}$ ($\mathbb{R}^n$ in the general setting). In the rest of the paper, we will abuse notations and use d to compare a given function $g \in F_{\mathcal{T}}$ to γ, even though γ is only defined on $\mathcal{T}$ and not on an interval of $\mathbb{R}$.

In most ODE integration methods, the approximation error depends on an integration step. We therefore introduce a discretization $\mathcal{D}_h$ of the time interval $[0, T]$, which we assume, for simplicity, to admit a constant step $h > 0$:

$$\mathcal{D}_h = \{0 = \tau_0, \tau_1, \tau_2, \ldots, \tau_J = T\}, \tag{9}$$

with $J > 0$ and $\tau_{j+1} - \tau_j = h$ for all $0 \leq j < J$.

For each parameter value $\boldsymbol{\lambda} \in \mathbf{W}$, the chosen approximation method will compute an approximate solution to the ODE, which we denote $y^{\boldsymbol{\lambda}}$. Similarly, the exact solution to Equation (1) such that $x(0) = x_0$ is denoted $x^{\boldsymbol{\lambda}}$.

For the sake of measuring the approximation error between $y^{\boldsymbol{\lambda}}$ and $x^{\boldsymbol{\lambda}}$, we use a finer notion of distance than the one proposed above. Indeed, standard integration methods provide guarantees that depend on the integration step in the sense that choosing a finer integration step enhances the quality of the approximation. Our aim here is to be able to take advantage of this fact, which could not be captured if we used the distance d from Equation (8).

Definition 3.1 (Global approximation error). Let $h > 0$ be the integration step of the chosen integration method. The *global approximation error* $\varepsilon_h(\boldsymbol{\lambda})$ between the approximate solution $y^{\boldsymbol{\lambda}}$ and the exact solution $x^{\boldsymbol{\lambda}}$ is defined as follows:

$$\varepsilon_h(\boldsymbol{\lambda}) = \max_{\tau \in \mathcal{D}_h} \left| x^{\boldsymbol{\lambda}}(\tau) - y^{\boldsymbol{\lambda}}(\tau) \right| . \tag{10}$$

In the rest of the paper, we make two assumptions on the approximation method. First, we assume that the set $\mathcal{T}$ of time points given by Equation (5), at which the set γ of observations is given, satisfies $\mathcal{T} \subset \mathcal{D}_h$. This assumption is quite natural as the set γ is finite, therefore a sufficiently small h can always be chosen accordingly. Second, we assume that the approximation method is *convergent*, which guarantees that for all $\boldsymbol{\lambda} \in \mathbf{W}$, the global approximation error $\varepsilon_h(\boldsymbol{\lambda})$ converges to 0 when h gets smaller. This assumption is directly satisfied for usual approximation methods (such as, e.g., Runge-Kutta; see for instance [7]).

3.2 Monte-Carlo method

We now move to our first result, i.e. providing an estimation of the probability that the original ODE system, with a given parameter value $\boldsymbol{\lambda}^*$, agrees with the experimental data with statistical guarantees. We then show in Section 3.3 how these results can be extended to reward functions.

Let $\boldsymbol{\lambda}^* \in \mathbf{W}$ be a parameter value. In order to take the internal variability of our system into account, we will consider that $\boldsymbol{\lambda}^*$ can slightly vary. In this regard, we set a constant $\rho > 0$ and consider the open ball

$$B(\boldsymbol{\lambda}^*, \rho) = \{\boldsymbol{\lambda} \in \mathbb{R}^m \mid \|\boldsymbol{\lambda} - \boldsymbol{\lambda}^*\|_{\mathbb{R}^m} < \rho\}, \tag{11}$$

where $\|\cdot\|_{\mathbb{R}^m}$ is the Euclidian norm defined in Section 2.1.

We start by recalling the Monte-Carlo procedure for estimation. This procedure aims at taking advantage of the Central Limit Theorem and the Law of Large Numbers. In order to estimate the probability that our system (where $\boldsymbol{\lambda}$ can vary inside of $B(\boldsymbol{\lambda}^*, \rho)$) satisfies a given property φ, we will generate a set of N samples of values for $\boldsymbol{\lambda}$ inside of $B(\boldsymbol{\lambda}^*, \rho)$, and use these values to provide N solutions to the ODE system. Each solution will be evaluated, yielding a score of 1 if it satisfies φ and 0 otherwise. Informally, the Central Limit Theorem (Theorem 3.2) states that the mean value of the samples $\hat{p}$ is a good estimator for the probability p that our system (defined in Equation (1)) satisfies φ. Moreover, it also provides a confidence interval that solely depends on the number of samples—provided this number is large enough—and the variance of the initial distribution.

Theorem 3.2 (Central Limit Theorem [36]). *Let $X_1, X_2, \ldots$ be a sequence of independent and identically distributed random variables of mean μ and variance σ^2. Then, the distribution of $\frac{\sum_{i=1}^{N} X_i - N\mu}{\sigma\sqrt{N}}$ converges to the standard normal distribution as $N \to \infty$. That is, for any $a \in \mathbb{R}$,*

$$\lim_{N\to\infty} \mathbb{P}\left(\frac{\sum_{i=1}^{N} X_i - N\mu}{\sigma\sqrt{N}} \leq a\right) = \frac{1}{\sqrt{2\pi}} \int_{-\infty}^{a} e^{-x^2/2} dx.$$

Let φ be a property to be checked on an ODE system. We want to compute the probability that the system satisfies φ, but we cannot evaluate the exact solutions of the ODE system. Since we have to rely on approximate solutions, we will define two auxiliary properties φ_-^ε and φ_+^ε that take into account the global approximation error defined above. We will then use the Monte-Carlo procedure to estimate two probabilities $\hat{p}_-^\varepsilon$ and $\hat{p}_+^\varepsilon$ using those properties and the approximate solutions, and propose an estimation of $\hat{p}$ that relies on $\hat{p}_-^\varepsilon$ and $\hat{p}_+^\varepsilon$. We will finally use $\hat{p}$ in order to evaluate the chosen (central) parameter value $\boldsymbol{\lambda}^*$.

Let $\mathcal{T}$ be a set of time points as described in Equation (5). Let γ be a set of observations and let $\delta > 0$ be a precision (tolerance) w.r.t. γ. Let $\boldsymbol{\lambda}^* \in \mathbf{W}$ be a parameter value, and let $\rho > 0$ be a variability setting. Consider the ball $\mathcal{B}_{\boldsymbol{\lambda}^*} = B(\boldsymbol{\lambda}^*, \rho)$ and let $\mathbb{P}^{\boldsymbol{\lambda}^*}$ be the uniform distribution on this ball.

Given a function $g \in F_{\mathcal{T}}$, we write $\varphi(g) := d(g, \gamma) \leq \delta$ for the property that means "the distance between g and γ is less than δ". For convenience, if $y^{\boldsymbol{\lambda}}$ is an approximate solution to Equation (1) induced by the parameter $\boldsymbol{\lambda} \in \mathcal{B}_{\boldsymbol{\lambda}^*}$, we will identify $\varphi(\boldsymbol{\lambda})$ to $\varphi(y^{\boldsymbol{\lambda}})$.

Given $\varepsilon > 0$, we introduce the properties:

$$\varphi(x^{\boldsymbol{\lambda}}) := d(x^{\boldsymbol{\lambda}}, \gamma) \leq \delta,$$
$$\varphi_-^\varepsilon(y^{\boldsymbol{\lambda}}) := d(y^{\boldsymbol{\lambda}}, \gamma) \leq \delta - \varepsilon, \quad \text{and} \quad \varphi_+^\varepsilon(y^{\boldsymbol{\lambda}}) := d(y^{\boldsymbol{\lambda}}, \gamma) \leq \delta + \varepsilon.$$

Our aim is to provide an estimation $\hat{p}$ for $\mathbb{P}^{\boldsymbol{\lambda}^*}(\varphi)$. For convenience, we write $\mathbb{P}$ for $\mathbb{P}^{\boldsymbol{\lambda}^*}$ in the rest of this section.

To this end, we show in Lemma 3.3 that for a small enough integration step h, we have $\varepsilon_h(\boldsymbol{\lambda}) \leq \varepsilon$ for all $\boldsymbol{\lambda} \in \mathcal{B}_{\boldsymbol{\lambda}^*}$, and therefore

$$\varphi_-^\varepsilon(y^{\boldsymbol{\lambda}}) \Rightarrow \varphi(x^{\boldsymbol{\lambda}}) \Rightarrow \varphi_+^\varepsilon(y^{\boldsymbol{\lambda}}). \tag{12}$$

Lemma 3.3. *Let $(h_i)_{i\in\mathbb{N}} \in \mathbb{R}^+$ be a sequence of integration steps, such that $\lim_{i\to\infty} h_i = 0$. Then for all $\varepsilon > 0$, there exists $i^* > 0$ such that*

$$\varepsilon_{h_i}(\boldsymbol{\lambda}) < \varepsilon, \quad \forall i \geq i^*, \forall \boldsymbol{\lambda} \in \mathcal{B}_{\boldsymbol{\lambda}^*}. \tag{13}$$

Roughly speaking, the global error $\varepsilon_h(\boldsymbol{\lambda})$ can be uniformly bounded in the closure $\overline{\mathcal{B}_{\boldsymbol{\lambda}^*}}$ of the open ball $\mathcal{B}_{\boldsymbol{\lambda}^*}$. The proof of this lemma is given in Appendix A.

Remark. Given a target approximation error ε, it is possible, depending on the integration schema, to compute a satisfactory h such that $\varepsilon_h < \varepsilon$. In our case, Runge-Kutta schemes have been thoroughly studied (see [28] for instance) and this approximation error can be bounded in terms of the successive derivatives of the function f involved in Equation (1), up to order 4. Similar methods can be found for other integration schemes. Here, if there exist L and M such that

$$\|f(x,t)\|_{\mathbb{R}} \leq M, \qquad \|f_{x^i t^j}\|_{\mathbb{R}} \leq L^{i+j}/M^{j-1} \tag{14}$$

where $f_{x^i t^j} = \frac{\partial^{i+j} f}{\partial^i x \partial^j t}$ is the $(i+j)$th derivative of f with respect to x and t, it is found that, for a one-dimensional system,

$$\|\varepsilon_h\|_{\mathbb{R}} \leq \frac{73}{720} M L^4 h^5. \tag{15}$$

In practice, it is the case since f is a regular function which we study on a compact space. Note that Equation (14) may be adapted to problems of any dimension by deriving f with respect to each components x_i of x and solving Equation (13) in [28].

Now, we define the probabilities

$$p = \mathbb{P}\big(\varphi(x^{\boldsymbol{\lambda}^*})\big), \quad p_-^\varepsilon = \mathbb{P}\big(\varphi_-^\varepsilon(y^{\boldsymbol{\lambda}^*})\big), \text{ and } p_+^\varepsilon = \mathbb{P}\big(\varphi_+^\varepsilon(y^{\boldsymbol{\lambda}^*})\big). \tag{16}$$

Note that p, p_- and p_+ implicitly depend on δ. However, we omit this dependence in order to lighten our notations. Next, it is straightforward that

$$p_-^\varepsilon \leq p \leq p_+^\varepsilon, \quad \forall \varepsilon > 0. \tag{17}$$

Estimators $\hat{p}_-^\varepsilon$ and $\hat{p}_+^\varepsilon$ of the probabilities p_-^ε and p_+^ε respectively can be determined using the Monte-Carlo procedure, involving a precision α and a risk θ. Our main result, given in Theorem 3.4 below, establishes a statistical guarantee on the probability p of interest with respect to these estimators $\hat{p}_-^\varepsilon$ and $\hat{p}_+^\varepsilon$.

Theorem 3.4 (Stability w.r.t. structural parameter). *Let $\boldsymbol{\lambda}^* \in \mathbf{W}$ be a parameter to be evaluated, and let ball radius $\rho > 0$, stability tolerance $\delta > 0$ and integration error $\varepsilon > 0$ be the different simulation settings. For any risk $\xi \in (0,1)$, we define $\theta = 1 - \sqrt{1-\xi}$. Then, for any precision $\alpha > 0$, the probabilities p_-^ε and p_+^ε defined in Equation (16) satisfy*

$$\mathbb{P}\big(p_-^\varepsilon \in [\hat{p}_-^\varepsilon - \alpha, \hat{p}_-^\varepsilon + \alpha]\big) \geq 1-\theta, \quad \mathbb{P}\big(p_+^\varepsilon \in [\hat{p}_+^\varepsilon - \alpha, \hat{p}_+^\varepsilon + \alpha]\big) \geq 1-\theta, \tag{18}$$

where the estimators $\hat{p}_-^\varepsilon$ and $\hat{p}_+^\varepsilon$ can each be determined after performing a number $N' = \frac{\log(2/\theta)}{2\alpha^2}$ (and hence a total number $N = 2 \times \frac{\log(2/\theta)}{2\alpha^2}$) of simulations of Equation (1) induced by the parameter values $\boldsymbol{\lambda}$ sampled uniformly in $\mathcal{B}_{\boldsymbol{\lambda}^*}$.

Furthermore, there exist $\varepsilon_0 > 0$ and $h_0 > 0$ sufficiently small such that, for any integration step $h \leq h_0$ and any $\varepsilon < \varepsilon_0$, the following statements hold:

- *The probability p defined in Equation (16) satisfies the estimation*

$$\mathbb{P}\big(p \in [\hat{p}_-^\varepsilon - \alpha, \hat{p}_+^\varepsilon + \alpha]\big) \geq 1-\xi. \tag{19}$$

- *The distance between $\hat{p}_-^\varepsilon$ and $\hat{p}_+^\varepsilon$ satisfies:*

$$\mathbb{P}\left(\left|\hat{p}_-^\varepsilon - \hat{p}_+^\varepsilon\right| \leq 3\alpha\right) \geq 1-\xi. \tag{20}$$

We emphasize that estimations (19) and (20) imply a confidence interval of width 5α for p and require a number of samples $N = 2 \times \frac{\log(2/\theta)}{2\alpha^2}$. If the analysis were performed directly on the exact solutions of the ODE, we would have a confidence interval of width 2α and only require $N = \frac{\log(2/\xi)}{2\alpha^2}$ samples.

The proof of Theorem 3.4, given in Appendix B, is divided in three main steps. First, using the Central Limit Theorem and the Law of Large Numbers, we determine estimators $\hat{p}_-^\varepsilon$ and $\hat{p}_+^\varepsilon$ of p_-^ε

and p_+^ε, respectively. Then, Equation (16) and the independence of simulations lead to the confidence interval of p. Finally, Lemma 3.3 guarantees that proper values of h and ε can be found, in order to control the distance between $\hat{p}_-^\varepsilon$ and $\hat{p}_+^\varepsilon$. It is worth noting that, for some integration methods (such as Runge-Kutta 4 for example), a value for h can be explicitly determined to guarantee Lemma 3.3 for a given ε and therefore Equation (19). However, the convergence speed of $\left|\hat{p}_-^\varepsilon - \hat{p}_+^\varepsilon\right|$ is not known in general, therefore we can only guarantee the existence of a sufficiently small value for ε to ensure Equation (20) but not compute it.

3.3 Model checking extension through reward functions

As explained in Section 2.3, our method can be extended to non-Boolean reward functions. Indeed, these functions may provide not only qualitative results—"does the property hold?"—but also *quantitative* ones—"*how well* does the property hold?". In our case, this allows to distinguish the good parameters that induce a suitable solution from the best ones that induce the solutions closest to the observations.

To use such a real-valued reward function r, some conditions are required. First, it must be assumed that two other reward functions r_- and r_+ can be found, such that they generalize Equation (17); in other words, the following estimation must hold for any $\boldsymbol{\lambda} \in \mathcal{B}_{\mathcal{\lambda}^*}$:

$$r_-(\boldsymbol{\lambda}) \leq r(\boldsymbol{\lambda}) \leq r_+(\boldsymbol{\lambda}). \tag{21}$$

Second, the law of the unconscious statistician must be applicable to these lower and upper reward functions, i.e. the computation of the expected value[2] must be applicable, so that estimators $\hat{r}_-$ and $\hat{r}_+$, of r_- and r_+ respectively, can be computed.

Moreover, and most importantly, the reward function must be *compatible* with the global error defined in Equation (10). Indeed, since we compute a score based on approximated solutions, these computations must take this approximation into account to provide any significance to the resulting score. It is worth noting that these conditions are satisfied by all the reward functions we have considered in this work, such as the total accumulated / maximal / average distance to γ or the number of time points where γ is not respected.

Similarly to Equation (20), the distance between $\hat{r}_-$ and $\hat{r}_+$ must be controlled. Depending on the order of the approximation method used to compute approximate solutions to the ODEs, this may be easy to ensure. For instance, in our case the integration method Runge-Kutta 4 ensures that the approximation error—and thus, the global error as defined in Equation (10)—is of order 5: all derivatives of the integration functions converge at most linearly w.r.t. h^5, where h is the integration step.

3.4 Case study: a study on *Aurelia Aurita* population growth [31]

In this section, we apply our method to a case study taken from the literature [31] to show its potential. After presenting the study and its conclusions, we will display our results and discuss them.

Context. In 2014, Melica et al. [31] published a paper studying the growth of a population of *Aurelia Aurita* individuals, a species of jellyfish that is very common in the Adriatic Sea. In that paper, they compared experimental data, resulting from the culture of *Aurelia Aurita* polyps, to simulation models based on the following ODE:

$$\frac{\mathrm{d}x(t)}{\mathrm{d}t} = ax(t)(1 - \frac{x(t)}{b}) \tag{22}$$

[2]See Equation (43) in Appendix B.

where t is time, x is the population density, a is the maximum rate of population growth, and b is the positive equilibrium. The authors have shown that the dynamics of an *Aurelia Aurita* polyps population can, indeed, be modeled by the density-dependent, or Verhulst [42], ODE presented above. They computed the values for a and b that ensure the best fitting w.r.t. the experimental data. More precisely, they chose to minimize the residual least square error $\chi^2 = \sum_k |x(t_k) - x_k|^2$. These values are presented in Table 1, where HD and LD represent the studies for *High* and *Low Density*, respectively, which were both ran by the original authors. Here, we focused on the *High Density* case.

	HD	*LD*
b	$5.35 \pm 0.11 (^{***}p < 0.001)$	$1.81 \pm 0.08 (^{***}p < 0.001)$
$x(0)$	$7.59 \pm 0.21 (^{***}p < 0.001)$	$0.081 \pm 0.017 (^{***}p < 0.001)$
a	$0.130 \pm 0.033 (^{**}p = 0.002)$	$0.137 \pm 0.012 (^{***}p < 0.001)$
χ^2	0.775	0.056

Table 1. Estimation of parameters of the logistic curve fitting the laboratory experimental data [31].

To illustrate our method, we applied it to the same case study, using Equation (22) as the ODE system and the provided data as observations.

Experiment. We now briefly recall the experiment. After discretizing the value space $\mathbf{W}$ defined in Equation (3) for the parameter $\boldsymbol{\lambda}$, we will evaluate every value in order to select the best ones w.r.t. the set γ of observations. To take the internal variability of the model into account, each chosen parameter value $\boldsymbol{\lambda}^*$ is associated with the open ball $\mathcal{B}_{\boldsymbol{\lambda}^*}$ as defined in Equation (11). Once the SMC parameters α and ξ, as well as a small enough value for ε are chosen, we can compute an integration step h, as well as a required number N of samples such that Theorem 3.4 holds. Then, we sample N values $\boldsymbol{\lambda} \in \mathcal{B}_{\boldsymbol{\lambda}^*}$, compute the approximated solutions to the induced ODEs, and compare them with the set γ of observations. For each $\boldsymbol{\lambda}^* \in \mathbf{W}$, we thus estimate the probabilities $\hat{p}^{\varepsilon}_{-}$ and $\hat{p}^{\varepsilon}_{+}$ defined in the previous section, and define $\text{grade}(\boldsymbol{\lambda}^*) = \hat{p}^{\varepsilon}_{-}$, which is the more constraining scenario. To better discriminate the best parameter values, we also estimate the expected value of the reward function $r : \boldsymbol{\lambda} \mapsto d(x^{\boldsymbol{\lambda}}, \gamma)$ that measures the distance between the ODE simulations and the experimental data. We implemented our technique in C++ to validate the approach. The experiments were realized on a 2.1 GHz Intel Xeon Silver 4216 processor, running g++ version 7.5.0 on Ubuntu 18.04. The code is available at https://gitlab.com/davidjulien/smc_for_ode.git, and the experiments can be reproduced using the right branches, i.e. *compute_aurelia* to run the experiment of Section 3.4.

We evaluated parameter values in the ranges $a \in [0, 3], b \in [0, 9]$, and discretized this space with a parameter step equal to 0.01. We set the internal variability of the parameters $\rho = 0.005\sqrt{2}$ and performed $N = 874$ simulations for each parameter value on the discretized space, ensuring a statistical precision $\alpha = 0.05$ and risk $\xi = 0.05$, using the Runge-Kutta 4 integration method. We targeted an error $\varepsilon = 0.01$, since this is the precision of the provided data. Using Equation (14), we chose $M = 7$ and $L = 7$. Then, we computed h using Equation (15): we found $\frac{73}{720} ML^4 h^5 \leq 0.01 \Leftrightarrow h \leq 0.089$, and picked $h = 0.08$. The computations completed in 52 minutes on 56 threads.

Results. In Figure 3, we represent the score of the best parameter values, in which the pink zones are zones where $\text{grade}(\boldsymbol{\lambda}^*) = 0$. As we can see, the gradient is strong and doesn't allow discrimination between values in this area. In order to refine the result, we present in Figure 4 the estimation of the expected value of the reward function $r : \boldsymbol{\lambda} \mapsto d(x^{\boldsymbol{\lambda}}, \gamma)$. Figure 4 shows a tighter

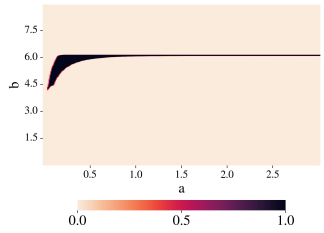

Fig. 3. Heatmap of the score of the parameters.

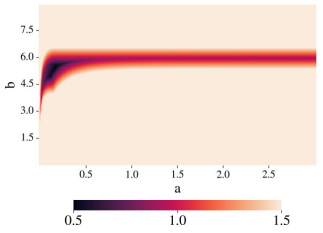

Fig. 4. Heatmap of the distance to γ.

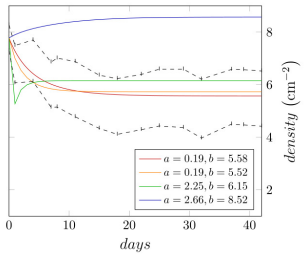

Fig. 5. Traces of models induced by the ODE from Equation (22) with different parameter values.

area of values that induce solutions that are very close to the data (down to 0.50 polyps on average), plotted in dark purple, which contains the parameter value $(a = 0.13, b = 5.35)$ estimated by [31]: it comforts us in saying that our method provides tangible results. The best parameter found using our method is the pair $(a = 0.19, b = 5.58)$: it induces the red curve in Figure 5.

4 STATISTICAL MODEL CHECKING FOR STABILITY ANALYSIS

In this section, we extend the result of Section 3 to provide statistical guarantees on properties related to the initial condition of an ODE system. Namely, given a property Γ (resp. the corresponding reward function r_Γ) on the initial condition of Equation (23), we will establish confidence intervals regarding the estimation of the *probability* of satisfaction of that property (resp. the *expected* value of r_Γ), which shall be computed using *approximate solutions* to Equation (23), as well as a bound on the errors w.r.t. the *exact probability* corresponding to the *exact solutions* to Equation (23).

First, we recall some definitions and propose a definition for stability. Next, we provide a method for estimating the probability p that the exact solution of our ODE system satisfies a given property Γ, using an estimator $\hat{p}$ that takes the approximation error into account. Finally, we illustrate our approach with another case study taken from the literature, by experimentally exhibiting the basin of attraction of a given ODE system.

Note that the numerical integration methods are the same as those defined in Section 3.1. We will slightly modify some definitions so that they refer to the initial condition x_0 of the system instead of its structural parameter $\boldsymbol{\lambda}$, and provide similar guarantees as in Section 3.2. From here and until the end of the section, we declare $\boldsymbol{\lambda}$ to be a constant, and we identify the pair $(x_0, \boldsymbol{\lambda}) \in \mathsf{INIT}$ to x_0. To lighten notations, we will remove $\boldsymbol{\lambda}$ from the different equations as it is not relevant in this section.

4.1 Stability

We consider the following Cauchy problem:

$$\begin{cases} \frac{\mathrm{d}x(t)}{\mathrm{d}t} = f(x(t)), \\ x(0) = x_0. \end{cases} \tag{23}$$

This Cauchy problem is related to an autonomous nonlinear system, where $x(t) \in \mathcal{X} \subseteq \mathbb{R}^n$, $\mathcal{X}$ is an open set, and $f : \mathcal{X} \mapsto \mathbb{R}^n$ is a continuous vector field on $\mathcal{X}$. Suppose that f has an equilibrium $x_e \in \mathcal{X}$, such that $f(x_e) = 0$. We first recall the mathematical definition of two forms of stability, which we aim at studying:

Definition 4.1 (Stability). The equilibrium x_e is said to be **Lyapunov stable** [29] if, for every $\zeta > 0$, there exists $\rho > 0$ such that $\|x(0) - x_e\|_{\mathbb{R}^n} < \rho \Rightarrow \|x(t) - x_e\|_{\mathbb{R}^n} \leq \zeta, \forall t \geq 0$. The equilibrium x_e is said to be **asymptotically stable** if it is Lyapunov stable and there exists $\rho > 0$ such that $\|x(0) - x_e\|_{\mathbb{R}^n} < \rho \Rightarrow \lim_{t\to\infty} \|x(t) - x_e\|_{\mathbb{R}^n} = 0$.

In order to be able to verify such notions with SMC techniques, we propose a weaker notion of stability. We start by only considering a finite interval $[T_1, T_2]$, with $T_1 < T_2$. Then, we propose the following notion of (ρ, ζ)-stability on $[T_1, T_2]$:

Definition 4.2 ((ρ, ζ)-stability). Let $d(\cdot, \cdot)$ be a distance between two functions of $\mathbb{R}^n$. Let $\rho > 0$ and $\zeta > 0$, then (x, x_0) be a solution to a differential system. This solution is called (ρ, ζ)-*stable* if, given another solution (x', x'_0) to this system

$$\left\|x_0 - x'_0\right\|_{\mathbb{R}^n} \leq \rho \Rightarrow d(x, x') \leq \zeta. \tag{24}$$

Since ζ is the tolerance of the method in the context of stability, we will write it δ.

Here, the observations consist in the equilibrium x_e, which we will compare to the trace obtained for a solution (x, x_0).

In this logic, (ρ, δ)-stability amounts to checking whether the property Γ holds for all initial conditions x_0 such that $\|x_0 - x_e\|_{\mathbb{R}^n} \leq \rho$. Computing the probability amounts to measuring the ratio of accepted initial conditions, i.e. the values which induce models whose trace satisfies Definition 4.2.

We now move to the computation of this probability and the associated statistical guarantees.

4.2 Upper bound on the approximation error

Let ρ be a positive real number. Similarly to Equation (11), we call $B_{\mathbb{R}^n}(a, \rho)$ the open ball of center $a \in \mathbb{R}^n$ and radius ρ for the canonical distance $\|\cdot\|_{\mathbb{R}^n}$ on $\mathbb{R}^n$. In the following, we assume the existence of an equilibrium x_e to f (defined in Equation (23)). Let $x_0^* \in \mathbf{V}$ be an initial condition to be checked. We lighten the notation and use $\mathcal{B}_{x_0^*} = B_{\mathbb{R}^n}(x_0^*, \rho)$, and use the distance $d(\cdot, \cdot)$ defined in Equation (8).

Given $\delta > 0$ and $\varepsilon > 0$, we define the following properties:

$$\begin{gathered} \Gamma(x_0) := d(x, x_e) \leq \delta, \\ \Gamma^{\varepsilon}_{-}(x_0) := d(x, x_e) \leq \delta - \varepsilon, \quad \text{and} \quad \Gamma^{\varepsilon}_{+}(x_0) := d(x, x_e) \leq \delta + \varepsilon. \end{gathered} \tag{25}$$

For any solution (x, x_0) to Equation (23) such that $x_0 \in \mathcal{B}_{x_0^*}$, Γ translates to "the solution (x, x_0) to Equation (23) is at distance δ from x_e, at most."

As in Section 3, we use the discretization $\mathcal{D}_h$ introduced in Equation (9) for the time interval $[T_1, T_2]$, which we assume, for simplicity, to admit a constant step $h > 0$:

$$\mathcal{D}_h = \{T_1 = \tau_0, \tau_1, \tau_2, \ldots, \tau_J = T_2\}, \tag{26}$$

where $J \in \mathbb{N}^*$ and $\tau_{j+1} - \tau_j = h$ for all $0 \leq j < J$.

For each initial condition value $x_0 \in \mathcal{B}_{x_0^*}$, the chosen approximation method will compute an approximate solution to the ODE, which we denote y^{x_0}. Recall that for any $x_0 \in \mathcal{B}_{x_0^*}$, the exact solution to Equation (23) such that $x(0) = x_0$ is written x^{x_0}.

We adapt the definition of global approximation error given in Equation (10), so that it refers to the initial condition x_0 rather than the structural parameter $\boldsymbol{\lambda}$:

$$\varepsilon_h(x_0) = \max_{\tau \in \mathcal{D}_h} \left| x^{x_0}(\tau) - y^{x_0}(\tau) \right|. \tag{27}$$

Again, the study of the stability of a set of values depends on our ability to find an upper bound on the global approximation error $\varepsilon_h(x_0)$. Such a bound exists on $\mathcal{B}_{x_0^*}$ thanks to the following Lemma:

Lemma 4.3. *Let x_e be an equilibrium for f in Equation (23), then $\rho > 0$. Let $(h_i)_{i\in\mathbb{N}} \in \mathbb{R}_+$ be a sequence of integration steps, such that $\lim_{h\to\infty} h_i = 0$. Then for all $\varepsilon > 0$, there exists i^* such that*

$$\varepsilon_{h_i}(x_0) < \varepsilon, \forall i \geq i^*, \forall x_0 \in \mathcal{B}_{x_0^*}. \tag{28}$$

Roughly speaking, Lemma 4.3 states the global approximation error $\varepsilon_h(x_0)$ can be uniformly bounded in the closure $\overline{\mathcal{B}_{x_0^*}}$ of the open ball $\mathcal{B}_{x_0^*}$. The proof is given in Section 1 of the supplementary materials.

Remark. Following the remark on Lemma 3.3, we can also bound the approximation error for two-dimensional systems. More precisely, given L and M such that

$$|f(x,t)|_{\mathbb{R}^2} \leq M, \qquad |f_{x_1^i x_2^j t^k}|_{\mathbb{R}^2} \leq L^{i+j+k}/M^{i+j-1} \tag{29}$$

where $f_{x_1^i x_2^j t^k} = \frac{\partial^{i+j+k} f}{\partial^i x_1 \partial^j x_2 \partial^k t}$ is the $(i+j+k)$th derivative of f with respect to x_1, x_2 and t, it is found that, for a two-dimensional system,

$$|\varepsilon_h|_{\mathbb{R}^2} \leq \frac{973}{720} M L^4 h^5. \tag{30}$$

Now, we can define the probabilities as follows:

$$p = \mathbb{P}\big(\Gamma(x^{x_0^*})\big), \quad p_-^\varepsilon = \mathbb{P}\big(\Gamma_-^\varepsilon(y^{x_0^*})\big), \text{ and } p_+^\varepsilon = \mathbb{P}\big(\Gamma_+^\varepsilon(y^{x_0^*})\big). \tag{31}$$

As in Section 3.2, we omit the dependence on δ for p, p_-^ε and p_+^ε. Again, estimators $\hat{p}_-^\varepsilon$ and $\hat{p}_+^\varepsilon$ of the probabilities p_-^ε and p_+^ε respectively can be determined using the Monte-Carlo procedure, involving a precision α and a risk θ; since it is the same procedure as Section 3.2, we will not go into details. We introduce the corresponding Theorem 4.4, which establishes a statistical guarantee on the probability p of interest w.r.t. the estimators $\hat{p}_-^\varepsilon$ and $\hat{p}_+^\varepsilon$.

Theorem 4.4 (Stability w.r.t. initial condition). *Let $x_0^* \in \mathbf{V}$ be an initial condition to be evaluated, and let $\rho > 0$, $\delta > 0$ and $\varepsilon > 0$ be the different simulation settings. For any risk $\xi \in (0,1)$, we define $\theta = 1 - \sqrt{1-\xi}$. Then, for any precision $\alpha > 0$, the probabilities p_-^ε and p_+^ε defined in Equation (31) satisfy*

$$\mathbb{P}\big(p_-^\varepsilon \in [\hat{p}_-^\varepsilon - \alpha, \hat{p}_-^\varepsilon + \alpha]\big) \geq 1-\theta, \quad \mathbb{P}\big(p_+^\varepsilon \in [\hat{p}_+^\varepsilon - \alpha, \hat{p}_+^\varepsilon + \alpha]\big) \geq 1-\theta, \tag{32}$$

where the estimators $\hat{p}_-^\varepsilon$ and $\hat{p}_+^\varepsilon$ can each be determined after performing a number $N' = \frac{\log(2/\theta)}{2\alpha^2}$ (and hence a total number $N = 2 \times \frac{\log(2/\theta)}{2\alpha^2}$) of simulations of Equation (23) induced by initial condition values x_0 sampled in $\mathcal{B}_{x_0^*}$.

Furthermore, there exist $\varepsilon_0 > 0$ and $h_0 > 0$ sufficiently small such that, for any integration step $h \leq h_0$ and any $\varepsilon < \varepsilon_0$, the following statements hold:

- *The probability p defined in Equation (31) satisfies the estimation*

$$\mathbb{P}\big(p \in [\hat{p}_-^\varepsilon - \alpha, \hat{p}_+^\varepsilon + \alpha]\big) \geq 1-\xi. \tag{33}$$

- *The distance between $\hat{p}_-^\varepsilon$ and $\hat{p}_+^\varepsilon$ satisfies:*

$$\mathbb{P}\left(\left|\hat{p}_-^\varepsilon - \hat{p}_+^\varepsilon\right| \leq 3\alpha\right) \geq 1-\xi. \tag{34}$$

Again, the estimations (33) and (34) imply a confidence interval of width 5α for p and require a number of samples $N = 2 \times \frac{\log(2/\theta)}{2\alpha^2}$. If the analysis were performed directly on the exact solutions of the ODE, we would have a confidence interval 2α and only require $N = \frac{\log(2/\xi)}{2\alpha^2}$ samples.

The proof of Theorem 4.4, given in Section 2 of the supplementary materials, is an adaptation of the proof of Theorem 3.4, and follows the same steps. Note that despite their similarity, we decided to separate Lemma 3.3 and Theorem 3.4 from Lemma 4.3 and Theorem 4.4 to follow mathematical conventions. Indeed, mainly for historical reasons, the behaviors of an ODE with respect to a variation of the parameter (i.e. bifurcation theory) or with respect to the initial condition (i.e. Lyapunov theory) are usually treated separately.

4.3 Case study: a study on Duffing's oscillator [13, 23]

Context. Duffing's oscillator, introduced in his book [13], is a non-linear second order equation used to model damped and driven oscillators. The equation is:

$$\frac{\mathrm{d}^2x(t)}{\mathrm{d}t^2} + a\frac{\mathrm{d}x(t)}{\mathrm{d}t} + bx(t) + dx(t)^3 = c\cos kt, \tag{35}$$

where a controls the amount of damping, b controls the linear stiffness, d controls the amount of non-linearity in the restoring force, c is the amplitude of the periodic driving force and k is the angular frequency of the periodic driving force. It is a well-studied system [20, 33, 44] and a primary example of chaotic behavior. In [23], the authors focus on a slightly modified oscillator equation:

$$\frac{\mathrm{d}^2x(t)}{\mathrm{d}t^2} + a\frac{\mathrm{d}x(t)}{\mathrm{d}t} + cx^2\frac{\mathrm{d}x(t)}{\mathrm{d}t} + bx(t) + dx(t)^3 = 0. \tag{36}$$

After rewriting it as a first-order system, we obtain the following two-dimensional system:

$$\begin{cases} \frac{\mathrm{d}x_1(t)}{\mathrm{d}t} &= x_2(t), \\ \frac{\mathrm{d}x_2(t)}{\mathrm{d}t} &= -bx_1(t) - ax_2(t) - dx_1(t)^3 - cx_1(t)^2x_2(t). \end{cases} \tag{37}$$

Experiments. The system exhibits very different behaviors depending on the value of (a, b, c, d), as we can see in Secttion 4.3.3 ; we will first focus on the study of the behavior for $(a, b, c, d) = (1, 1, -1, -1)$: this parameter set has already been theoretically studied and induces a system which has two equilibria located at $x_{e,1} = (-1, 0)$ and $x_{e,2} = (1, 0)$.

Again, the experiments were realized on a 2.1 GHz Intel Xeon Silver 4216 processor, running g++ version 7.5.0 on Ubuntu 18.04. The code is available at https://gitlab.com/davidjulien/smc_for_ode.git, and the experiments can be reproduced using the right branches, i.e. *compute_stability* to run the experiment of Section 4.3.1, and *compute_basin* to run the experiment of Section 4.3.2. Results of Section 4.3.3 may be obtained by changing the value of a in the branch *compute_basin*. We used the Runge-Kutta 4 method to compute approximate solutions. Since the system is very sensitive, we needed a very low approximation error. We targeted an error $\varepsilon = 10^{-12}$. Using Equation (29), we chose $M = 18$ and $L = 2$. Then, we computed h using Equation (30): we found $\frac{973}{720}ML^4h^5 \leq \varepsilon \Leftrightarrow h \leq 0.0012$. We picked an integration step $h = 0.001$. The computations completed in 3 hours and 19 minutes on 56 threads.

4.3.1 Experimental evidence of a basin of attraction. Let $x_e \in \mathbb{R}^n$ be an equilibrium for the system presented in Equation (37). In this section, we want to experimentally exhibit (ρ, δ)-stability around x_e, that is, given $\delta > 0$, finding a radius $\rho > 0$ such that every $x_0 \in \mathcal{B}_{x_e} = B_{\mathbb{R}^n}(x_e, \rho)$ satisfies the property Γ defined in Equation (25).

Symbolic analysis predicts that $x_{e,1} = (-1, 0)$ and $x_{e,2} = (1, 0)$ are such equilibria, so we will conduct the analysis on those two values even though we could look for stability at any point

$x_s \in \mathbb{R}^2$. We picked $\delta = 1$ and evaluated initial condition values in the balls $B_{\mathbb{R}^n}(x_e, \rho_i)$ for $\rho_i = 0.001 + i \times 0.01$, $\rho_i \leq 2$. Note that those values are completely arbitrary. We performed $N = 874$ simulations for each ball, ensuring a statistical precision $\alpha = 0.05$ and a risk $\xi = 0.05$.

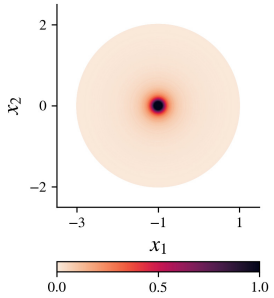

Fig. 6. Heatmap of the score of the initial conditions, relative to $x_{e,1} = (-1, 0)$.

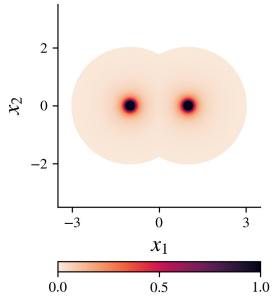

Fig. 7. Heatmap of the score of the initial conditions, relative to both $x_{e,1}$ and $x_{e,2}$.

Results. In Figure 6, the color represents the score $\text{grade}(\mathcal{B}_{x_e,\rho_i})$ of the concentric balls $\mathcal{B}_{x_e,\rho_i}$ regarding the property $\Gamma(x_0) = \text{d}(x, x_e) < 1$, where $0 \leq \rho_i \leq 2, x_0 \in \mathcal{B}_{x_e,\rho_i}$ and (x, x_0) is a solution to Equation (35): the darker the circle, the higher the score (i.e. the bigger the ratio of accepted simulations). The figure shows darker zones around the value $x_{e,1} = (-1, 0)$, which highlights that the system is stable around $x_{e,1}$. The lighter zones show balls $\mathcal{B}_{x_e,\rho}$ for which $\text{grade}(\mathcal{B}_{x_e,\rho})$ is close to 0, which indicates that the system is less, if not, stable in such a large zone. The white zones are zones where we did not perform simulations. After performing the same study on $x_{e,2} = (1, 0)$, we can combine the two studies to depict the stability behavior of the system regarding both equilibria at once: this is presented in Figure 7. The figure clearly shows the two stable zones around $x_{e,1}$ and $x_{e,2}$, as predicted in [23]. We also experimentally gained knowledge regarding the basins of attraction for the system, especially that there are at least two of them, that they are disconnected, along with a rough estimation of their width.

As in Section 3.4, one can see that there is a small gradient in the areas where the score is positive, but this not enough to discriminate values. To obtain more precise information on the stability of the system, we will now present the study regarding the estimation of the distance between the induced traces and the equilibria.

4.3.2 Experimental delimitation of a basin of attraction. Now that stability is experimentally exhibited, we want to address a more complicated problem from an analytical point of view: getting the shape of the basin of attraction. To do that, as explained in Section 3.3, we will use reward functions and perform a study that is similar to what we did in Section 3.4: we will discretize the space of initial conditions and, for each value, compute the expected distance of the induced trace to the equilibrium by performing numerous simulations in its vicinity.

This time, we analyzed a portion $\mathcal{I} = [-2, 2] \times [-1.5, 1.5]$ of the plan, using a discretization step equal to 0.01. Again, by performing $N = 874$ simulations for each value and for each property, we guarantee a statistical precision $\alpha = 0.05$ and a risk $\xi = 0.05$.

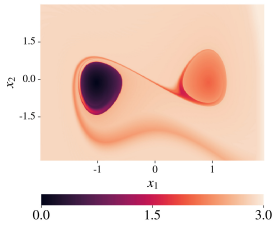

Fig. 8. Heatmap of the stability of the left equilibrium $x_{e,1} = (-1, 0)$.

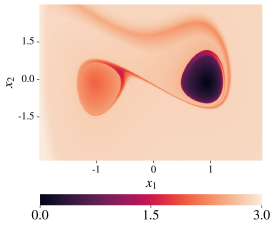

Fig. 9. Heatmap of the stability of the right equilibrium $x_{e,2} = (1, 0)$.

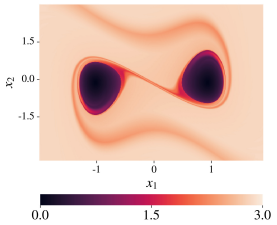

Fig. 10. Heatmap of the stability of the system, relative to both $x_{e,1}$ and $x_{e,2}$.

Results. In Figure 8, we represent the estimation of the reward function $r : x_0 \mapsto d(x^{x_0}, x_e)$, where d is the distance defined in Equation (8) and x_e is the left equilibrium of Equation (37). In other words, we depict the expected distance to x_e of the trace induced by each discrete value in $\mathcal{I}$: the darker the point, the closer the trace of the induced model is expected to be to the equilibrium. One can see the ovoid shape of dark purple on the left, which is consistent with the expected behavior of the system in this portion of the space: again, this comforts us in saying that our method provides tangible results. The same study regarding the right equilibrium is plotted in Figure 9, which is a point reflection through $(0, 0)$ of Figure 8. Both studies show a darker orange zone a the position of the converse equilibrium: this was also expected, since in this region the system is also stable, but w.r.t. the other equilibrium. Thus, the system will stay in the vicinity of said equilibrium, effectively maintaining its distance to the studied equilibrium.

Finally, Figure 10 shows a combination of the two former studies, exhibiting the minimal expected distance to either one of the two equilibria $x_{e,1}$ and $x_{e,2}$, effectively defining the shape of stability of the system. Again, this is consistent with the theoretical analysis of the system, which predicts a "bow-tie" shape for the basin of attraction. We emphasize that these shapes are *discrete*: we may only have a finite precision on the border of the basin of attraction ; increasing the discretization step would yield better precision, at the cost of greatly increasing the computation time. Therefore, we had to settle on a compromise.

4.3.3 Influence of the structural parameter on the shape of the basin of attraction. In this section, we provide some material on the study of the influence of the structural parameter $\boldsymbol{\lambda}$ on the shape of the basin of attraction. We perform the same analysis as in Section 4.3.2 for different values of the structural parameter. The results of these analysises are given in Figures 11 to 15, and the meaning of the colors is the same as in Section 4.3.2: the darker the spot, the closer the induced trace is expected to be to the equilibria.

Results. As we can see in Figures 11 to 15, the parameter a has a direct influence on the shape of the basin of attraction: the basin of attraction gets narrower as a decreases. Again, this is consistent with the theoretical study [23] of the system. Note that this is preliminary work: we do not have the mathematical guarantees, regarding the global error ε, offered in the rest of the paper when both the structural parameter $\boldsymbol{\lambda}$ and the initial condition x_0 vary.

5 CONCLUSION

In this paper, we have proposed a statistical method for synthesizing both structural parameter and initial condition values w.r.t. a given set of observations for an ODE system with internal variability, while providing formal statistical guarantees that for the first time (to the best of our knowledge)

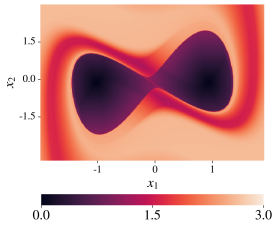

Fig. 11. Heatmap of the stability of the system, $\boldsymbol{\lambda} = (-0.8, -1, 1, 1)$.

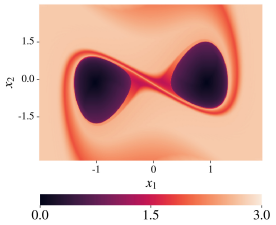

Fig. 12. Heatmap of the stability of the system, $\boldsymbol{\lambda} = (-0.9, -1, 1, 1)$.

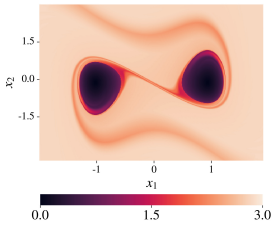

Fig. 13. Heatmap of the stability of the system, $\boldsymbol{\lambda} = (-1, -1, 1, 1)$.

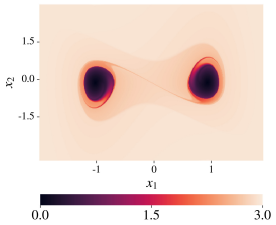

Fig. 14. Heatmap of the stability of the system, $\boldsymbol{\lambda} = (-1.1, -1, 1, 1)$.

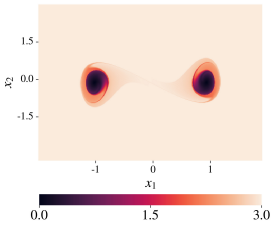

Fig. 15. Heatmap of the stability of the system, $\boldsymbol{\lambda} = (-1.2, -1, 1, 1)$.

take into account the approximation error introduced through the numerical integration of the ODEs. To do that, we discretize the value space and define balls around each element of the resulting (finite) set to take internal variability into account. We then use the Monte-Carlo technique to estimate the probability that exact solutions to the ODE system are close to the observations for each ball, and use the result of this estimation to select the best (central) values. In the context of parameterization, this corresponds to selecting the parameter value that induces a model that fits best with experimental data under variability; in the context of stability analysis, it allows to exhibit the basin of attraction of equilibria under variability. Our contributions for parameterization and stability analysis are Theorems 3.4 and 4.4 respectively, which guarantee the precision of our estimation for each value to be tested despite the fact that it is performed using numerical integration techniques that do not give us access to exact solutions of the ODE system. We also show in the corresponding Lemmas 3.3 and 4.3 that an upper bound on the integration step of the chosen integration technique exists (and can be computed for standard integration techniques) in order to make sure that a given statistical precision and risk are respected. In contrast with other existing works on parameter estimation for ODE systems, like [27], where this problem is left aside, we show that the number of simulations required for a given precision and risk of the statistical estimation is more than twice the one needed when working with exact solutions.

One of the limitations of our work is that, in order to prove our results, we rely on a setting ε that represents the maximal admissible distance between exact and approximate solutions to the ODE system. While it is possible, for most integration techniques, to compute an integration step that will guarantee that a given value for ε is respected [3], our results only show the existence of a suitable value for ε for any statistical setting and do not provide any method to compute this value

[3]See Appendix A, and [28].

in practice. This is due to our lack of guarantees on the convergence speed of the distance between the two estimators $\hat{p}^{\epsilon}_{-}$ and $\hat{p}^{\epsilon}_{+}$ that appear in Equations 20 and 34. A third limitation exposed in Section 4.3.3 is that we have no result regarding the study of both the parameter $\boldsymbol{\lambda}$ and the initial condition x_0 at the same time. While the first experiments are consistent with the theoretical analysis [23], the statistical results obtained in Theorems 3.4 and 4.4 may not be trivially combined, and their combination deserves a proper analysis.

The inclusion of solvers such as [6, 34] may be of great interest, as it would allow combining their guarantees regarding floating point computation error with our guarantees on approximation error. However, since our results are limited to the ODE integration, the comparison would not be relevant considering the advance of our work.

Our work can be extended by considering hybrid models that exhibit both continuous and discrete dynamic behavior. Most formal verification tasks on these models are undecidable [21], but the experimental nature of SMC allows for other kinds of verification. A second extension could be to use our method to study stochastic models defined with stochastic ODE systems. These two types of model are, to the best of our knowledge, yet to be theoretically studied so that similar, if not corresponding, results obtained via experimental methods can be guaranteed. To be able to study this type of models would allow scientists to get results on stochastic processes such as Brownian motion in the case of astrophysics [32] or stock prices [5], as well as dynamical hybrid systems which may be described with stochastic hybrid automata [8].

As mentioned in Section 1, we emphasize that our results are generic and could therefore be implemented for any system for which we have the sufficient guarantees, including models which are too difficult to analyze symbolically. Moreover, our technique can be combined with any exploration strategy for the value space. The global exploration we perform in this paper is obviously costly but yields global information that is precious when analyzing a complex system. In the future, we plan on combining a coarse global exploration to identify interesting zones in the value space with more efficient and detailed search algorithms (such as the one from [27]) limited to those zones. In this regard, adaptative discretization, as used in [15], looks promising.

REFERENCES

[1] Julien Alexandre dit Sandretto and Alexandre Chapoutot. 2016. Validated Explicit and Implicit Runge-Kutta Methods. In *Reliable Computing*, Vol. 22. 79–103.

[2] Julien Alexandre dit Sandretto and Jian Wan. 2018. Reachability Analysis of Nonlinear ODEs Using Polytopic Based Validated Runge-Kutta, In Reachability Problems. *SpringerLink*, 1–14. https://doi.org/10.1007/978-3-030-00250-3_1

[3] Christel Baier, Luca de Alfaro, Vojtěch Forejt, and Marta Kwiatkowska. 2018. Model checking probabilistic systems. In *Handbook of Model Checking*. Springer, 963–999. https://doi.org/10.1007/978-3-319-10575-8_28

[4] Ran Bao, Christian Attiogbe, Benoît Delahaye, Paulin Fournier, and Didier Lime. 2019. Parametric statistical model checking of UAV flight plan. In *International Conference on Formal Techniques for Distributed Objects, Components, and Systems*. Springer, 57–74. https://doi.org/10.1007/978-3-030-21759-4_4

[5] Fischer Black and Myron Scholes. 1973. The Pricing of Options and Corporate Liabilities. *Journal of Political Economy* (May 1973). https://doi.org/10.1086/260062

[6] Olivier Bouissou and Matthieu Martel. 2006. GRKLib: a Guaranteed Runge Kutta Library, In 12th GAMM - IMACS International Symposium on Scientific Computing, Computer Arithmetic and Validated Numerics (SCAN 2006). *12th GAMM - IMACS International Symposium on Scientific Computing, Computer Arithmetic and Validated Numerics (SCAN 2006)*, 8. https://doi.org/10.1109/SCAN.2006.20

[7] John Charles Butcher. 2016. *Numerical methods for ordinary differential equations*. John Wiley & Sons. https://doi.org/10.1002/9781119121534 Third Edition.

[8] G. A. Pérez Castañeda, J.-F. Aubry, and N. Brinzei. 2011. Stochastic hybrid automata model for dynamic reliability assessment. *Proceedings of the Institution of Mechanical Engineers, Part O: Journal of Risk and Reliability* 225, 1 (March 2011), 28–41. https://doi.org/10.1177/1748006XJRR312

[9] Michel Crouzeix and Alain L Mignot. 1984. *Analyse numérique des équations différentielles*. Vol. 1. Masson.

[10] Conrado Daws. 2004. Symbolic and parametric model checking of discrete-time Markov chains. In *International Colloquium on Theoretical Aspects of Computing*. Springer, 280–294. https://doi.org/10.1007/978-3-540-31862-0_21

[11] Christian Dehnert, Sebastian Junges, Nils Jansen, Florian Corzilius, Matthias Volk, Harold Bruintjes, Joost-Pieter Katoen, and Erika Ábrahám. 2015. Prophesy: A probabilistic parameter synthesis tool. In *International Conference on Computer Aided Verification*. Springer, 214–231. https://doi.org/10.1007/978-3-319-21690-4_13

[12] Jean-Pierre Demailly. 2012. *Analyse numérique et équations différentielles*. EDP Sciences.

[13] Georg Duffing and Fritz Emde. 1918. *Erzwungene Schwingungen bei veränderlicher Eigenfrequenz und ihre technische Bedeutung*. Vieweg.

[14] Nelson Dunford and Jacob Theodore Schwartz. 1967. *Linear operators. 1. General theory*. Interscience Publishers.

[15] Christian Ellen, Sebastian Gerwinn, and Martin Fränzle. 2015. Statistical model checking for stochastic hybrid systems involving nondeterminism over continuous domains. *International Journal on Software Tools for Technology Transfer* 17, 4 (Aug. 2015), 485–504. https://doi.org/10.1007/s10009-014-0329-y

[16] Paul Gainer, Ernst Moritz Hahn, and Sven Schewe. 2018. Accelerated model checking of parametric Markov chains. In *International Symposium on Automated Technology for Verification and Analysis*. Springer, 300–316. https://doi.org/10.1007/978-3-030-01090-4_18

[17] Benjamin M. Gyori, Bing Liu, Soumya Paul, R. Ramanathan, and P.S. Thiagarajan. 2015. Approximate probabilistic verification of hybrid systems. In *International Workshop on Hybrid Systems Biology*. Springer, 96–116. https://doi.org/10.1007/978-3-319-26916-0_6

[18] Jack K. Hale. 1980. *Ordinary Differential Equations*. R. E. Krieger Publishing Company.

[19] Tingting Han, Joost-Pieter Katoen, and Alexandru Mereacre. 2008. Approximate parameter synthesis for probabilistic time-bounded reachability. In *2008 Real-Time Systems Symposium*. IEEE, 173–182. https://doi.org/10.1109/RTSS.2008.19

[20] Chihiro Hayashi. 2014. *Nonlinear Oscillations in Physical Systems*. Princeton University Press, Princeton, NJ, USA. https://doi.org/10.1515/9781400852871

[21] Thomas A. Henzinger, Peter W. Kopke, Anuj Puri, and Pravin Varaiya. 1998. What's Decidable about Hybrid Automata? *J. Comput. System Sci.* 57, 1 (Aug. 1998), 94–124. https://doi.org/10.1006/jcss.1998.1581

[22] Wassily Hoeffding. 1963. Probability inequalities for sums of bounded random variables. *J. Amer. Statist. Assoc.* 58, 301 (1963), 13–30. https://doi.org/10.1080/01621459.1963.10500830

[23] P. Holmes and D. Rand. 1980. Phase portraits and bifurcations of the non-linear oscillator:$\ddot{x} + \alpha\dot{x} + \gamma x^2\dot{x} + \beta x + \delta x^3 = 0$. *International Journal of Non-Linear Mechanics* 15, 6 (Jan. 1980), 449–458. https://doi.org/10.1016/0020-7462(80)90031-1

[24] David Julien, Guillaume Cantin, and Benoît Delahaye. 2022. End-to-End Statistical Model Checking for Parametric ODE Models. In *QEST: International Conference on Quantitative Evaluation of Systems (Lecture Notes in Computer Science, Vol. 13479)*, Erika Ábrahám and Marco Paolieri (Eds.). Springer International Publishing, Warsaw, Poland, 85–106. https://doi.org/10.1007/978-3-031-16336-4_5

[25] Joost-Pieter Katoen. 2016. The probabilistic model checking landscape. In *Proceedings of the 31st Annual ACM/IEEE Symposium on Logic in Computer Science*. 31–45. https://doi.org/10.1145/2933575.2934574

[26] Axel Legay, Benoît Delahaye, and Saddek Bensalem. 2010. Statistical model checking: An overview. In *International Conference on Runtime Verification*. Springer, 122–135. https://doi.org/10.1007/978-3-642-16612-9_11

[27] B. Liu, B. M. Gyori, and P. S. Thiagarajan. 2019. *Statistical model checking-based analysis of biological networks*. Springer International Publishing, 63–92. https://doi.org/10.48550/arXiv.1812.01091

[28] Max Lotkin. 1951. On the accuracy of Runge-Kuttaś method. *Math. Tables Aids Comput.* 5, 35 (1951), 128–133. https://doi.org/10.1090/S0025-5718-1951-0043566-3

[29] Aleksandr Mikhallovich Lyapunov. 1992. *General problem of the stability of motion*. Taylor & Francis.

[30] John Maidens and Murat Arcak. 2014. Trajectory-based reachability analysis of switched nonlinear systems using matrix measures, In 53rd IEEE Conference on Decision and Control. *53rd IEEE Conference on Decision and Control*, 6358–6364. https://doi.org/10.1109/CDC.2014.7040386

[31] Valentina Melica, Sergio Invernizzi, and Gabriella Caristi. 2014. Logistic density-dependent growth of an Aurelia aurita polyps population. *Ecological Modelling* 291 (2014), 1–5. https://doi.org/10.1016/j.ecolmodel.2014.07.009

[32] David Merritt. 2013. *Dynamics and Evolution of Galactic Nuclei*. Princeton University Press, Princeton, NJ, USA. https://press.princeton.edu/books/hardcover/9780691121017/dynamics-and-evolution-of-galactic-nuclei

[33] Nicholai Minorsky. 1962. *Nonlinear Oscillations*. Van Nostrand.

[34] N. S. Nedialkov. 2006. Interval Tools for ODEs and DAEs, In 12th GAMM - IMACS International Symposium on Scientific Computing, Computer Arithmetic and Validated Numerics (SCAN 2006). *12th GAMM - IMACS International Symposium on Scientific Computing, Computer Arithmetic and Validated Numerics (SCAN 2006)*, 4. https://doi.org/10.1109/SCAN.2006.28

[35] Lawrence Perko. 2013. *Differential equations and dynamical systems*. Springer New York. https://doi.org/10.1007/978-1-4613-0003-8

[36] Valentin Vladimirovitch Petrov. 1975. *Sums of independent random variables.* De Gruyter. https://doi.org/10.1515/9783112573006
[37] Andreas Podelski and Silke Wagner. 2006. Model Checking of Hybrid Systems: From Reachability Towards Stability. In *Hybrid Systems: Computation and Control*, João P. Hespanha and Ashish Tiwari (Eds.). Springer Berlin Heidelberg, Berlin, Heidelberg, 507–521. https://doi.org/10.1007/11730637_38
[38] Pavithra Prabhakar and Miriam Garcia Soto. 2013. Abstraction Based Model-Checking of Stability of Hybrid Systems. In *Computer Aided Verification*, Natasha Sharygina and Helmut Veith (Eds.). Springer Berlin Heidelberg, Berlin, Heidelberg, 280–295. https://doi.org/10.1007/978-3-642-39799-8_20
[39] Simon Ramondenc, Damien Eveillard, Lionel Guidi, Fabien Lombard, and Benoît Delahaye. 2020. Probabilistic modeling to estimate jellyfish ecophysiological properties and size distributions. *Scientific Reports* 10, 1 (2020), 1–13. https://doi.org/10.1038/s41598-020-62357-5
[40] Jim O Ramsay, Giles Hooker, David Campbell, and Jiguo Cao. 2007. Parameter estimation for differential equations: A generalized smoothing approach. *Journal of the Royal Statistical Society: Series B (Statistical Methodology)* 69, 5 (2007), 741–796. https://doi.org/10.1111/j.1467-9868.2007.00610.x
[41] Fedor Shmarov and Paolo Zuliani. 2016. Probabilistic Hybrid Systems Verification via SMT and Monte Carlo Techniques, In Hardware and Software: Verification and Testing. *SpringerLink*, 152–168. https://doi.org/10.1007/978-3-319-49052-6_10
[42] John H. Vandermeer and Deborah E. Goldberg. 2013. Population ecology. In *Population Ecology*. Princeton University Press.
[43] Qinsi Wang, Paolo Zuliani, Soonho Kong, Sicun Gao, and Edmund M. Clarke. 2015. SReach: A Probabilistic Bounded Delta-Reachability Analyzer for Stochastic Hybrid Systems, In Computational Methods in Systems Biology. *SpringerLink*, 15–27. https://doi.org/10.1007/978-3-319-23401-4_3
[44] W. Weaver, Jr., S. P. Timoshenko, and D. H. Young. 1991. *Vibration Problems in Engineering, 5th Edition.* Wiley, Hoboken, NJ, USA. https://www.wiley.com/en-us/Vibration+Problems+in+Engineering%2C+5th+Edition-p-9780471632283

A PROOF OF LEMMA 3.3

First, we recall the definition of *stability* of an approximation method.

Definition A.1 (Method stability). We say that the approximation method determined by Equation (7) is stable if there exists a constant $\mathcal{K} > 0$, called *stability constant*, such that, for any two sequences $(y_k)_{0\leq k\leq J}$ and $(\widetilde{y}_k)_{0\leq k\leq J}$ defined as $y_{k+1} = y_k + h\,\Phi(\tau_k, y_k, \boldsymbol{\lambda}, h)$ and $\widetilde{y}_{k+1} = \widetilde{y}_k + h\,\Phi(\tau_k, \widetilde{y}_k, \boldsymbol{\lambda}, h) + \eta_k$ respectively, $(0 \leq k < J)$, with $\boldsymbol{\lambda} \in \mathbf{W}$ and $\eta_k \in \mathbb{R}$, we have

$$\max_{0\leq k\leq J} \|y_k - \widetilde{y}_k\|_{\mathbb{R}^n} \leq \mathcal{K}\big(\|y_0 - \widetilde{y}_0\|_{\mathbb{R}^n} + \sum_{0\leq k\leq J} |\eta_k| \big). \tag{38}$$

Note that this stability is relative to the method: it does not imply stability of the studied system itself.

It is well-known that if Φ is κ-Lipschitz w.r.t. y, *i.e.* $\forall t \in [0,T]$, $\forall y_1, y_2 \in \mathbb{R}$, $\forall \boldsymbol{\lambda} \in \mathbf{W}$ and $\forall h \in \mathbb{R}$, $\|\Phi(t, y_1, \boldsymbol{\lambda}, h) - \Phi(t, y_2, \boldsymbol{\lambda}, h)\|_{\mathbb{R}^n} \leq \kappa \|y_1 - y_2\|_{\mathbb{R}^n}$, then stability is ensured (see for instance [7] or [9]).

Now, we fix $\boldsymbol{\lambda}^* \in \mathbf{W}$ and $\boldsymbol{\lambda}_1, \boldsymbol{\lambda}_2 \in \mathcal{B}_{\boldsymbol{\lambda}^*}$, and we consider the approximate solutions $y^{\boldsymbol{\lambda}_1}, y^{\boldsymbol{\lambda}_2}$ to Equation (1) relative to $\boldsymbol{\lambda}_1$ and $\boldsymbol{\lambda}_2$ and starting from x_0.

$$\begin{cases} y_0^{\boldsymbol{\lambda}_1} &= x_0, \\ y_{k+1}^{\boldsymbol{\lambda}_1} &= y_k^{\boldsymbol{\lambda}_1} + h\,\Phi(t_k, y_k^{\boldsymbol{\lambda}_1}, \boldsymbol{\lambda}_1, h), \end{cases} \quad \begin{cases} y_0^{\boldsymbol{\lambda}_2} &= x_0, \\ y_{k+1}^{\boldsymbol{\lambda}_2} &= y_k^{\boldsymbol{\lambda}_2} + h\,\Phi(t_k, y_k^{\boldsymbol{\lambda}_2}, \boldsymbol{\lambda}_2, h). \end{cases}$$

We recall that the exact solutions to Equation (1) relative to $\boldsymbol{\lambda}_1$ and $\boldsymbol{\lambda}_2$ and starting from x_0 are denoted $x^{\boldsymbol{\lambda}_1}$ and $x^{\boldsymbol{\lambda}_2}$ respectively. For $i \in \{1,2\}$ and $0 \leq k \leq J$, we introduce the consistency error on $y^{\boldsymbol{\lambda}_i}$ at step k:

$$\varepsilon_{h,k}(\boldsymbol{\lambda}_i) = \left\| x^{\boldsymbol{\lambda}_i}(\tau_k) - y^{\boldsymbol{\lambda}_i}(\tau_k) \right\|_{\mathbb{R}^n}. \tag{39}$$

The consistency errors satisfy $\varepsilon_h(\boldsymbol{\lambda}_i) = \max_{0\le k\le J} \varepsilon_{h,k}(\boldsymbol{\lambda}_i)$, for $i \in \{1,2\}$, where $\varepsilon_h(\boldsymbol{\lambda}_i)$ is the global approximation error (defined by Equation (10)). The proof of Lemma 3.3 can be derived from the following theorem:

Theorem A.2 (Stability with respect to consistency error). *Assume that the function Φ defined in Equation (7) is κ_1-Lipschitz w.r.t. $\boldsymbol{\lambda}$ and κ_2-Lipschitz continuous w.r.t. y. Then the approximation method is stable w.r.t. the consistency error,* i.e. *there exists $\mathcal{K} > 0$ such that*

$$\forall \boldsymbol{\lambda}_1, \boldsymbol{\lambda}_2 \in \mathcal{B}_{\boldsymbol{\lambda}^*}, \max_{0\le k\le J} \left|\varepsilon_{h,k}(\boldsymbol{\lambda}_1) - \varepsilon_{h,k}(\boldsymbol{\lambda}_2)\right| \le \mathcal{K} \left\|\boldsymbol{\lambda}_1 - \boldsymbol{\lambda}_2\right\|_{\mathbb{R}^m}. \tag{40}$$

where $\|\cdot\|$ is the Euclidean norm defined in Section 2.

Proof of Theorem A.2. By assumption, Φ is κ_1-Lipschitz continuous w.r.t. $\boldsymbol{\lambda}$:

$$\forall t, y, h \in \mathbb{R}, \forall \boldsymbol{\lambda}_1, \boldsymbol{\lambda}_2 \in \mathcal{B}_{\boldsymbol{\lambda}^*}, \left\|\Phi(t, y, \boldsymbol{\lambda}_1, h) - \Phi(t, y, \boldsymbol{\lambda}_2, h)\right\|_{\mathbb{R}^n} \le \kappa_1 \left\|\boldsymbol{\lambda}_1 - \boldsymbol{\lambda}_2\right\|_{\mathbb{R}^m}.$$

It follows that

$$\begin{aligned}
\left\|y_{k+1}^{\boldsymbol{\lambda}_1} - y_{k+1}^{\boldsymbol{\lambda}_2}\right\|_{\mathbb{R}^n} &\le \left\|y_k^{\boldsymbol{\lambda}_1} - y_k^{\boldsymbol{\lambda}_2}\right\|_{\mathbb{R}^n} + h\left\|\Phi(t_k, y_k^{\boldsymbol{\lambda}_1}, \boldsymbol{\lambda}_1, h) - \Phi(t_k, y_k^{\boldsymbol{\lambda}_2}, \boldsymbol{\lambda}_2, h)\right\|_{\mathbb{R}^n} \\
&\le \left\|y_k^{\boldsymbol{\lambda}_1} - y_k^{\boldsymbol{\lambda}_2}\right\|_{\mathbb{R}^n} + h\left\|\Phi(t_k, y_k^{\boldsymbol{\lambda}_1}, \boldsymbol{\lambda}_1, h) - \Phi(t_k, y_k^{\boldsymbol{\lambda}_1}, \boldsymbol{\lambda}_2, h)\right\|_{\mathbb{R}^n} \\
&\quad + h\left\|\Phi(t_k, y_k^{\boldsymbol{\lambda}_1}, \boldsymbol{\lambda}_2, h) - \Phi(t_k, y_k^{\boldsymbol{\lambda}_2}, \boldsymbol{\lambda}_2, h)\right\|_{\mathbb{R}^n} \\
&\le (1 + h\kappa_2)\left\|y_k^{\boldsymbol{\lambda}_1} - y_k^{\boldsymbol{\lambda}_2}\right\|_{\mathbb{R}^n} + h\kappa_1 \left\|\boldsymbol{\lambda}_1 - \boldsymbol{\lambda}_2\right\|_{\mathbb{R}^m},
\end{aligned}$$

for $0 \le k \le J$. We write $\left\|y_k^{\boldsymbol{\lambda}_1} - y_k^{\boldsymbol{\lambda}_2}\right\|_{\mathbb{R}^n} = \Delta_{y,k}$ and $\|\boldsymbol{\lambda}_1 - \boldsymbol{\lambda}_2\|_{\mathbb{R}^m} = \Delta_{\boldsymbol{\lambda}}$, and we get

$$\Delta_{y,k+1} \le (1 + h\kappa_2)\Delta_{y,k} + h\kappa_1\Delta_{\boldsymbol{\lambda}}. \tag{41}$$

Applying the discrete Gronwall Lemma (see for instance [12], VIII.2.3), we deduce

$$\max_{0\le k\le J} \Delta_{y,k} \le e^{\kappa_2 T}\big(\Delta_{y,0} + \sum_{0\le j\le k-1} h\kappa_1\Delta_{\boldsymbol{\lambda}}\big)$$

which leads to

$$\max_{0\le k\le J} \left\|y_k^{\boldsymbol{\lambda}_1} - y_k^{\boldsymbol{\lambda}_2}\right\|_{\mathbb{R}^n} \le e^{\kappa_2 T} T\kappa_1 \left\|\boldsymbol{\lambda}_1 - \boldsymbol{\lambda}_2\right\|_{\mathbb{R}^m},$$

since $y_0^{\boldsymbol{\lambda}_1} = y_0^{\boldsymbol{\lambda}_2} = x_0$ and $h\,J = T$.

Furthermore, it is proved in [9] that if Φ is Lipschitz continuous w.r.t. $\boldsymbol{\lambda}$, then the exact solution $x^{\boldsymbol{\lambda}}$ is also Lipschitz continuous w.r.t. $\boldsymbol{\lambda}$ that is, there exists $\kappa_3 > 0$ such that

$$\forall \boldsymbol{\lambda}_1, \boldsymbol{\lambda}_2 \in \mathcal{B}_{\boldsymbol{\lambda}^*}, \forall t \in [0, T], \left\|x^{\boldsymbol{\lambda}_1}(t) - x^{\boldsymbol{\lambda}_2}(t)\right\|_{\mathbb{R}^n} \le \kappa_3 \left\|\boldsymbol{\lambda}_1 - \boldsymbol{\lambda}_2\right\|_{\mathbb{R}^m}. \tag{42}$$

Finally, we have

$$\begin{aligned}
\left|\varepsilon_{h,k}(\boldsymbol{\lambda}_1) - \varepsilon_{h,k}(\boldsymbol{\lambda}_2)\right| &\le \left\|x^{\boldsymbol{\lambda}_1}(\tau_k) - y^{\boldsymbol{\lambda}_1}(\tau_k) - x^{\boldsymbol{\lambda}_2}(\tau_k) - y^{\boldsymbol{\lambda}_2}(\tau_k)\right\|_{\mathbb{R}^n} \\
&\le \left\|x^{\boldsymbol{\lambda}_1}(\tau_k) - x^{\boldsymbol{\lambda}_2}(\tau_k)\right\|_{\mathbb{R}^n} + \left\|y^{\boldsymbol{\lambda}_1}(\tau_k) - y^{\boldsymbol{\lambda}_2}(\tau_k)\right\|_{\mathbb{R}^n} \\
&\le \mathcal{K} \left\|\boldsymbol{\lambda}_1 - \boldsymbol{\lambda}_2\right\|_{\mathbb{R}^m},
\end{aligned}$$

with $\mathcal{K} = \kappa_3 + T\kappa_1 e^{\kappa_2 T}$, which completes the proof of Theorem A.2. □

It remains to show that Theorem A.2 implies Lemma 3.3.

Proof of Lemma 3.3. Let $(h_i)_{i\geq 0}$ be a sequence of discretization steps such that $\lim_{i\to\infty} h_i = 0$. Since the approximation method given by (7) is assumed to be convergent, each function $\varepsilon_{h_i}(\cdot)$ defined in Equation (39) is pointwise convergent to 0.

Furthermore, we recall that Φ is Lipschitz continuous w.r.t. $\boldsymbol{\lambda} \in \mathbf{W}$. Hence, Theorem A.2 implies that the functions $\left(\varepsilon_{h_i}(\cdot)\right)_{i\geq 0}$ defined in Equation (39) are also Lipschitz continuous, with uniform Lipschitz constant $\mathcal{K}$:

$$\left|\varepsilon_{h_i}(\boldsymbol{\lambda}_1) - \varepsilon_{h_i}(\boldsymbol{\lambda}_2)\right| \leq \mathcal{K}\|\boldsymbol{\lambda}_1 - \boldsymbol{\lambda}_2\|_{\mathbb{R}^m}, \quad \forall \boldsymbol{\lambda}_1, \boldsymbol{\lambda}_2 \in \mathcal{B}_{\boldsymbol{\lambda}^*}, \quad \forall i \in \mathbb{N}.$$

Consequently, the functions $\left(\varepsilon_{h_i}(\cdot)\right)_{i\geq 0}$ are uniformly equicontinuous. Hence, Arzelà–Ascoli Theorem [14] implies that the sequence $\left(\varepsilon_{h_i}(\cdot)\right)_{i\geq 0}$ converges uniformly to 0 on $\mathcal{B}_{\boldsymbol{\lambda}^*}$, thus $\forall \varepsilon > 0$, $\exists i^* \in \mathbb{N}, \forall i \geq i^*, \forall \boldsymbol{\lambda} \in \mathcal{B}_{\boldsymbol{\lambda}^*}, \varepsilon_{h_i}(\boldsymbol{\lambda}) < \varepsilon$, and Lemma 3.3 is proved. □

We emphasize that Lemma 3.3 can be supplemented by an explicit choice of a sufficiently small integration step h, provided the integration method comes with appropriate estimates of their global error. Notably, the accuracy of the Runge-Kutta 4 method, which we use for the numerical treatment of our case studies, has been thoroughly studied (see [28] for instance), and it is known that its inherent error can be bounded in terms of the successive derivatives of the function f involved in Equation (1), up to order 4.

B PROOF OF THEOREM 3.4

First step. We begin the proof of Theorem 3.4 by showing how to compute an estimator $\hat{p}^{\varepsilon}_{-}$ of the probability p^{ε}_{-} defined in (16).

Let $(\boldsymbol{\lambda}_i)_{\mathbb{N}}$ be a sequence of values in the ball $\mathcal{B}_{\boldsymbol{\lambda}^*}$. We write B_i the random variable corresponding to the test "$\varphi^{\varepsilon}_{-}(\boldsymbol{\lambda}_i)$ holds": all the B_i are i.i.d. variables and follow a Bernoulli's law of parameter p^{ε}_{-}. We write b_i the evaluation of B_i. We introduce the transfer function $g_- : \mathcal{B}_{\boldsymbol{\lambda}^*} \to \{0, 1\}$ corresponding to the test regarding $\varphi^{\varepsilon}_{-}(\boldsymbol{\lambda}_i)$, defined by $g_-(\boldsymbol{\lambda}_i) = 1$ if $\varphi^{\varepsilon}_{-}(\boldsymbol{\lambda}_i)$ holds, 0 otherwise. Next, we consider

$$G = \mathbb{E}(g_-(X)) = \int_{\mathcal{B}_{\boldsymbol{\lambda}^*}} g_-(\boldsymbol{\lambda}) f_X(\boldsymbol{\lambda}) \mathrm{d}\boldsymbol{\lambda}, \tag{43}$$

where f_X is defined by a uniform distribution, that is, $f_X(\boldsymbol{\lambda}) = \frac{1}{|\mathcal{B}_{\boldsymbol{\lambda}^*}|}$, $x \in \mathcal{B}_{\boldsymbol{\lambda}^*}$. We produce a sample $(\boldsymbol{\lambda}_1, \boldsymbol{\lambda}_2, \ldots, \boldsymbol{\lambda}_N)$ of the variable X in $\mathcal{B}_{\boldsymbol{\lambda}^*}$, and use it to compute the Monte-Carlo estimator G. By virtue of the Law of Large Numbers, the sample mean satisfies: $\overline{g}_N = \frac{1}{N}\sum_{i=1}^{N} g_-(\boldsymbol{\lambda}_i)$. The Central Limit Theorem states that the variable $Z = \frac{\overline{g}_N - G}{\sigma_{\overline{g}_N}}$ approximately follows a Standard Normal Distribution $\mathcal{N}(0, 1)$; hence, for a risk θ, we can bound the error $|\alpha_N|$ of swapping G with $\overline{g}_N$ by building confidence intervals:

$$\mathbb{P}\left(|\alpha_N| \leq \chi_{1-\frac{\theta}{2}} \frac{\sigma_{g_-}}{\sqrt{N}}\right) = 1 - \theta, \tag{44}$$

where $\chi_{1-\frac{\theta}{2}}$ is the quantile of the Standard Normal Distribution $\mathcal{N}(0, 1)$ and σ_{g_-} is the variance of g_-.

Since we are interested in finding p^{ε}_{-} with a certain confidence, we can perform this process after setting the desired target error α and risk θ, knowing how many simulations must be ran using Hoeffding's inequality [22]:

$$\theta = \mathbb{P}(\overline{g}_N \notin [p^{\varepsilon}_{-} - \alpha, p^{\varepsilon}_{-} + \alpha]) \leq 2\exp(-2\alpha^2 N),$$

or equivalently $N \geq \frac{\log(2/\theta)}{2\alpha^2}$. Here, it is worth emphasizing that N can be chosen independently of ε.

Further, the variance of $\overline{g}_N$ can be expressed with the variance of $g_-(X)$:

$$\sigma^2_{g_-} = \mathbb{E}\left([g_-(X) - \mathbb{E}(g_-(X))]^2\right) = \int_{\mathcal{B}_{\lambda^*}} (g_-(\boldsymbol{\lambda}))^2 f_X(\boldsymbol{\lambda}) \mathrm{d}\boldsymbol{\lambda} - G^2.$$

We consider i.i.d. samples, hence $\sigma^2_{g_-}$ can be estimated with the variance $S^2_{g_-}$:

$$\sigma^2_{g_-} \simeq S^2_{g_-} = \frac{1}{N}\sum_{i=1}^{N} (g_-(\boldsymbol{\lambda}_i)^2 - \overline{g}^2_N).$$

It follows that σ_{g_-} can be estimated with its empirical counterpart $\hat{\sigma}_{g_-} = \sqrt{S^2_{g_-}}$, which shows that the error displays a $1/\sqrt{N}$ convergence.

Finally, after estimating σ_{g_-}, we can find $\hat{p}^\varepsilon_-$ using the variance of Bernoulli's law $\hat{\sigma}^2_{g_-} = \hat{p}^\varepsilon_- \times (1 - \hat{p}^\varepsilon_-)$. We conclude that the probability that $\varphi^\varepsilon_-(\boldsymbol{\lambda})$ holds is estimated by $\hat{p}^\varepsilon_- = \frac{1}{2}\left(1 \pm \sqrt{1 - 4\hat{\sigma}^2_{g_-}}\right)$, with an error α and a risk θ, provided we perform $N \geq \frac{\log(2/\theta)}{2\alpha^2}$ simulations. It follows that

$$\mathbb{P}\big(p^\varepsilon_- \in [\hat{p}^\varepsilon_- - \alpha, \hat{p}^\varepsilon_- + \alpha]\big) \geq 1 - \theta. \tag{45}$$

Similarly, we determine an estimator $\hat{p}^\varepsilon_+$ of p^ε_+ by running $N \geq \frac{\log(2/\theta)}{2\alpha^2}$ additional simulations, and obtain a confidence interval satisfying

$$\mathbb{P}\big(p^\varepsilon_+ \in [\hat{p}^\varepsilon_+ - \alpha, \hat{p}^\varepsilon_+ + \alpha]\big) \geq 1 - \theta. \tag{46}$$

Second step. Now, let us show how a confidence interval for the probability p can be derived from the confidence intervals given in (45), (46), involving the estimators $\hat{p}^\varepsilon_-$ and $\hat{p}^\varepsilon_+$ respectively. The independence of the samples used to determine the estimators $\hat{p}^\varepsilon_-$, $\hat{p}^\varepsilon_+$ guarantees that

$$\mathbb{P}(p \in [\hat{p}^\varepsilon_- - \alpha, \hat{p}^\varepsilon_+ + \alpha]) = \mathbb{P}\big(\{p \geq \hat{p}^\varepsilon_- - \alpha\}\big) \times \mathbb{P}\big(\{p \leq \hat{p}^\varepsilon_+ + \alpha\}\big).$$

By virtue of (45), we have $\mathbb{P}(p^\varepsilon_- \geq \hat{p}^\varepsilon_- - \alpha) \geq 1 - \theta$. Next, the estimate (19) implies $\mathbb{P}(p \geq \hat{p}^\varepsilon_- - \alpha) \geq \mathbb{P}(p^\varepsilon_- \geq \hat{p}^\varepsilon_- - \alpha) \geq 1 - \theta$. Similarly, we have $\mathbb{P}(p \leq \hat{p}^\varepsilon_+ + \alpha) \geq 1 - \theta$, and finally $\mathbb{P}(p \in [\hat{p}^\varepsilon_- - \alpha, \hat{p}^\varepsilon_+ + \alpha]) \geq (1 - \theta)^2 = 1 - \xi$, since $\theta = 1 - \sqrt{1 - \xi}$.

Third step. Finally, let us prove how Lemma 3.3 guarantees that proper values of h and ε can be found, in order to control the distance between $\hat{p}_-$ and $\hat{p}_+$.

Indeed, the continuity of the probability measure $\mathbb{P}$ ensures that there exists $\varepsilon_0 > 0$ such that $\left|p^\varepsilon_- - p^\varepsilon_+\right| \leq \alpha$, for $\varepsilon < \varepsilon_0$. Next, we write

$$\left|\hat{p}^\varepsilon_- - \hat{p}^\varepsilon_+\right| \leq \left|\hat{p}^\varepsilon_- - p^\varepsilon_-\right| + \left|\hat{p}^\varepsilon_+ - p^\varepsilon_+\right| + \left|p^\varepsilon_- - p^\varepsilon_+\right|,$$

hence we have, for $\varepsilon < \varepsilon_0$:

$$\begin{aligned}\mathbb{P}\left(\left|\hat{p}^\varepsilon_- - \hat{p}^\varepsilon_+\right| \leq 3\alpha\right) &\geq \mathbb{P}\left(\left|\hat{p}^\varepsilon_- - p^\varepsilon_-\right| \leq \alpha\right) \times \mathbb{P}\left(\left|\hat{p}^\varepsilon_+ - p^\varepsilon_+\right| \leq \alpha\right) \times \mathbb{P}\left(\left|p^\varepsilon_- - p^\varepsilon_+\right| \leq \alpha\right) \\ &\geq (1 - \theta)^2 \times 1 = 1 - \xi.\end{aligned}$$

In parallel, Lemma 3.3 guarantees that for h sufficiently small, the global stability error can be uniformly bounded on $\mathcal{B}_{\lambda^*}$ by ε_0. The proof is complete. □